Chapter 4:

Genotypic and phenotypic study of antibiotic resistance in *K. pneumoniae*

4.1 Introduction

Klebsiella pneumoniae is a highly adaptable bacterium that is renowned for producing a broad range of illnesses, with urinary tract infections (UTIs) being especially common on a global scale. Additionally, it is involved in respiratory and bloodstream infections and is acknowledged as a member of a cohort of very potent and resistant bacteria (Foxman, 2010). The World Health Organization classifies it as a high-priority species because of the worldwide issue of antibiotic resistance. Uropathogenic strains of *K. pneumoniae* have distinct characteristics that facilitate their ability to colonize human cells and medical equipment. These properties include adhesins and the production of biofilms, which may complicate the treatment process. *K. pneumoniae* is categorized by the World Health Organization as a bacterium of concern regarding antibiotic resistance. This is due to its propensity to develop resistance to many kinds of antimicrobial agents, ranging from penicillins, cephalosporins, and quinolones, commonly employed in the treatment of *K. pneumoniae* infections (Rawat & Nair, 2010; L. Chen, Mathema, Chavda, et al., 2014; Henson et al., 2017).

The resistance is a result of genes that are present in both the chromosomes and plasmids. *Klebsiella pneumoniae* has gained a reputation as a significant facilitator of the transmission and development of antimicrobial resistance genes due to the large number of these genes found on plasmids and mobile genetic elements. This makes *K. pneumoniae* a crucial player in the transfer of AMR genes across different species of *Klebsiella* and other *Enterobacterales* (Wyres et al., 2020). ESBLs render nearly all beta-lactam antibiotics, including penicillins and cephalosporins, ineffective, with the exception of carbapenems. However, the most worrying issue is the rise in the occurrence of carbapenemase generating *K. pneumoniae* isolates (Annual Epidemiological Report, 2022), which severely restricts the available treatment choices and leads to outbreaks in hospitals that facilitate the further dissemination of antimicrobial resistance (Foxman, 2010; Perdigão et al., 2021).

Whole genome sequencing (WGS) has significantly transformed the field of pathogen research. It has not only allowed for the identification of mutations and plasmids linked with antimicrobial resistance (J. Phelan et al., 2016; J. E. Phelan et al., 2019), but also enabled the analysis of phylogenies and transmission events (Guerra-Assunção et al., 2015; Napier et al., 2020). The *K. pneumoniae* phylogeny often exhibits clades that align with the widely used multi-locus sequence typing method (MLST), which relies on seven gene loci (*gapA, mdh, infB, pgi, rpoB, phoE,* and

tonB) (Diancourt et al., 2005). Currently, there are a total of 7178 distinct STs that have been defined in the pasteurMLST databases (https://bigsdb.pasteur.fr/klebsiella/). Genotyping is crucial for the identification of cases or outbreaks caused by *K. pneumoniae* and for the subsequent tracing of the source and spread of infections (Guo et al., 2015). MLST is regarded as an effective technique for classifying bacterial infections. It is utilized to ascertain the genetic relationships across bacterial strains and to identify and track the global spread of drug-resistant strains (Maiden et al., 1998; Carvalho-Castro et al., 2017). MLST is essential for monitoring the disease transmission and antimicrobial resistance of *K. pneumoniae*. The MLST technique facilitates the identification of particular sequence types linked to virulence or resistance genes by predicting the evolutionary relationships among *K. pneumoniae* isolates (Rahmani et al., 2023). By comparing clinical isolates with a single nucleotide variation, it allows for precise characterisation of transmission and outbreaks. This method provides valuable information about the existence of resistance and virulence genes, as well as the genetic links between isolates (Gentile et al., 2020; Argimón et al., 2021; Foster-Nyarko et al., 2023).

β-lactams, including penicillins, cephalosporins, and carbapenems, are extensively utilized antibiotics for treating *Klebsiella* infections worldwide. Nevertheless, certain strains of bacteria can become resistant to such antimicrobial agents by accumulating plasmid-mediated extended-spectrum β-lactamases (ESBL), AmpC, and carbapenemase genes. Examples of these genes include *bla*CTX-M-15, *bla*SHV, *bla*CMY, *bla*TEM, *bla*DHA, *bla*NDM, *bla*OXA-48, *bla*KPC, *bla*VIM, and *bla*IMP. This resistance mechanism is widely recognized as one of the most significant dangers to global health (De Oliveira et al., 2020). Carbapenem resistance is a significant issue in healthcare-associated infections. Because there aren't many ways to treat carbapenem-resistant strains like carbapenem-resistant *K. pneumoniae* and other carbapenem-resistant *Enterobacteriaceae* (CRE), they have been labeled as "critical priority pathogens" (Papp-Wallace et al., 2010). Carbapenem resistance in *K. pneumoniae* can be caused by specific molecular processes such as carbapenemase synthesis, efflux pumps, and porin mutations (Pattolath et al., 2023).

The metallo-lactamase (NDM), a kind of carbapenemase, which poses a significant threat to global health, was initially identified in a Swedish patient who previously underwent medical treatment in India (Yong et al., 2009). NDM-5, initially identified in *E. coli*, exhibited a substitution of Valine at position 88 and Methionine at number 154 with Leucine (A. U. Khan et al., 2017). NDM-5

demonstrates more hydrolytic activity towards carbapenems, ceftazidime, cephalothin, and cefotaxime compared to NDM-1 (A. U. Khan et al., 2017). OXA-48 was discovered in 2001 after a patient in Istanbul, Turkey, developed carbapenem-resistant *K. pneumoniae*. The literature claims that the "OXA-48-like" subfamily developed following several variants in the oxacillinase-type enzyme OXA-48 since its initial discovery (Poirel et al., 2004). Different variants offer OXA-48 one to five amino acid changes or deletions. Two of the most well-known members are OXA-181 (four modifications at Thr104Ala, Asn110Asp, Glu168Gln, and Ser 171Ala) and OXA-232 (one substitution at Arg214Ser) (Pitout et al., 2019). In recent times, a limited number of investigations have demonstrated the existence of bacteria that produce two types of enzymes that confer resistance to carbapenem antibiotics, namely NDM and OXA (Shibl et al., 2013; Cho et al., 2015; Avolio et al., 2017; Solgi et al., 2020). Nonetheless, there is a lack of extensive research on the correlations between the genotypic presence of single and dual carbapenemase manufacturers and the phenotypic MIC values.

However, there exist additional genes that confer resistance to various kinds of antibiotics, including *aac, ant,* and *aph* genes for aminoglycosides; *acrAB, kdeA, OqxAB,* and *aa(6')-Ib-cr* for quinolones; *fos* for fosfomycin; and the *tet* gene for tetracycline resistance (Y. Li et al., 2023). Further, in case of colistin resistance, the Two Component System (TCS) *PhoPQ* and *PmrAB* are triggered by the loss of cations in the Outer Membrane, leading to the formation and transfer of phosphoethanolamine (pEtN) and 4-amino-4-deoxy-L-arabinose (L-Ara4N) cationic groups. These LPS alterations prevent colistin from binding and balance the negative charge on the outer membrane (Olaitan et al., 2014). Mutations in the genes of two component systems, *PhoPQ* and *PmrAB,* cause constitutive activation of the latter, which leads to colistin resistance (Miller et al., 2011; Olaitan et al., 2014; Aghapour et al., 2019). Also, the *mgrB* gene's inactivation's leads to colistin resistance in *K. pneumoniae* (Lopez-Camacho et al., 2014; Cannatelli et al., 2015).

The complicated molecular pathways driving tigecycline resistance include the overexpression of RND (resistance-nodulation-division) efflux pumps. Tigecycline-resistant efflux pump systems comprise *AcrAB-TolC* and its positive regulators, *SoxS, ramA, MarA*, or its negative regulator, *ramR* (Hentschke et al., 2010; Roy et al., 2013; Villa et al., 2014; H. Xu et al., 2016). The overexpression of *ramA* caused by an inactivating mutation in *ramR* raises the level of expression of the *AcrAB* pump genes, which in turn causes tigecycline resistance (Hentschke et al., 2010).

Few studies suggested that tigecycline and colistin resistance in *K. pneumoniae* may be largely caused by insertional inactivation in *ramR* and *mgrB* (Taniguchi et al., 2017).

Biofilm formation is an effective method used by bacteria to ensure their survival. This technique is particularly significant in the context of healthcare-associated infections (HAIs), especially those related to medical devices (Francolini & Donelli, 2010). *K. pneumoniae* can produce a significant amount of biofilm outside of its cells. This biofilm helps the bacteria stick to both living and non-living surfaces. This biofilm hinders the entry of antibiotics and reduces the effectiveness of drugs on the extracellular matrix (Nirwati et al., 2019). Temperate phages, also known as lysogenic phages, are viruses that undergo an alternate life cycle by integrating their genetic material into the host organism and become prophages. During this condition, the DNA of the phage undergoes replication alongside the host cell (known as lysogeny) and is preserved within the bacterial population. A comprehensive bacterial genomics has shown that a significant portion of bacterial DNA consists of prophage-like components and remains of prophages in some bacteria (Canchaya et al., 2003; Casjens, 2003).

The genome of *K. pneumoniae* contains three unique types of prophages: intact, questionable, and incomplete. These prophages are classified based on their completeness scores determined using PHASTER bioinformatics techniques. Regions with a total score below 70 are categorized as incomplete. A score falling within the range of 70 to 90 is classified as dubious. On the other hand, if the score is more than 90, it is categorized as Intact (Arndt et al., 2016). The use of lytic phages in phage treatment to specifically eliminate target bacteria has been hampered by regulatory barriers, limiting the progress of this therapeutic method. However, prophage induction therapy has the potential to be used in clinical settings to specifically target bacteria strains that are resistant to antibiotics. This therapy can be used as an alternative to present treatments that rely on antibiotics (Lakshminarasimhan, 2022b). *Klebsiella* genomes have a high frequency of prophages. *K. pneumoniae* is around the lower 5th percentile of the species with the highest prophage abundance (De Sousa et al., 2020). Despite the utilization of lytic phages in phage treatment to induce host-specific elimination of target bacteria, the advancement of this therapeutic approach has been impeded by regulatory obstacles. The potential application of prophage induction therapy in clinical settings involves targeting antibiotic-resistant strains of bacteria and utilizing it as an alternative to current antibiotic-based treatments (Lakshminarasimhan, 2022b).

Efficient monitoring and surveillance systems are essential for comprehending worldwide patterns and organizing synchronized efforts to counteract the spread of antibiotic resistance. So far, more than 400 genes that cause resistance to antimicrobial drugs have been discovered in *K. pneumoniae*, and the number of different versions of these genes is still increasing (Wyres et al., 2019, 2020). Whole-genome sequencing is an effective method for surveillance and tracking of antimicrobial resistance. It provides important information about the genetics of MDR and XDR respectively. This helps us better understand the genetic variables that contribute to antimicrobial resistance and virulence. WGS also allows us to study the spread and evolution of strains in healthcare settings (Cui et al., 2019). Most importantly, due to its decreasing price over the past few years, next-generation sequencing has emerged as a promising tool for simultaneous outbreak detection and surveillance (Mellmann et al., 2011).

This chapter primarily examines antibiotic resistance, specifically the monitoring of AMR genes using genome-based methods. The primary emphasis is on beta-lactamases, plasmids, and significant sequence types that are prevalent in India, as well as their relationship with antibiotic resistance. We also investigated the impact of dual carbapenemase on the increase in minimum inhibitory concentration. Further prophage induction therapy using lower concentrations of mitomycin C (MMC) was also attempted to overcome the challenges of resistant and virulent *K. pneumoniae*.

4.2 Materials and methodology

4.2.1 Pan-India *K. pneumoniae* genome data retrieval

The genomic sequences of multi-drug resistant *Klebsiella pneumoniae* (MDRKp), totaling 187 samples, were obtained from the PATRIC database (https://www.patricbrc.org/) up to February 2021. The genomes from India with antimicrobial resistance properties were accessed using filters such as 'Genome quality: good', 'India', and 'Antimicrobial resistance'. In December 2022, this database was consolidated with the Bacterial and Viral Bioinformatics Resource Center (https://www.bv-brc.org/). The high-quality, already assembled sequences in FASTA format were obtained and utilized for the comprehensive analysis together with our samples n = 22 (M2, M6, M10, M17B, M34a, M39, M40, M47, M48, M49, M50, M51, M52, M53, M54, M55, M56, M57,

M58, M59, DJ, and ST1). Information regarding strains, including the year of collection, sample origin, geographic area, and host health, was also gathered from PATRIC for each genome.

4.2.2 Multi-locus Sequence Typing

The metadata in the PATRIC database included MLST profiles for all isolates, except for a small number of them. Nevertheless, all the isolates were thoroughly reexamined for sequence typing in order to prevent any errors. To identify the sequence types, we employed MLST v2.0.4 from the Centre for Genomic Epidemiology (CGE) toolbox. The MLST tool can be accessible via the following URL: https://cge.cbs.dtu.dk/services/MLST/. The entry was recorded on November 17, 2021. To determine sequence types (STs), a combination of 7 housekeeping genes (*gapA, mdh, infB, phoE, rpoB, pgi, tonB*) and their allelic variations were utilized to generate the STs.

4.2.3 Screening for antimicrobial resistance genes and detecting their location

The isolates were analyzed to detect the presence of genes associated with antibiotic resistance. This was done by examining the Contig, ORF_ID, and Start and Stop positions in the genomes using the Resistance Gene Identifier (RGI) tool. The analysis focused on perfect and strict matches only, using the criteria from The Comprehensive Antibiotic Resistance Database (CARD). The research was performed utilizing the website at https://card.mcmaster.ca/analyze/rgi. The resistance score of each isolates was determined by using Kleborate tool available at https://cgps.gitbook.io/pathogenwatch/technical-descriptions/typing-methods/kleborate. To facilitate further investigation, the beta-lactamase genes among all the discovered genes were isolated. This is because beta-lactamase genes, specifically carbapenem and ESBLs, are the primary drivers of resistance in *K. pneumoniae*. Further, the mlplasmids v2.1.0 software was used to identify the position of β-lactamase genes in the genome. The software can be viewed at https://sarredondo.shinyapps.io/mlplasmids/.

4.2.4 Screening of plasmid replicons

Plasmids were identified using the PlasmidFinder v2.0.1 program from the CGE toolbox (https://cge.cbs.dtu.dk/services/PlasmidFinder/). The enterobacteriales database was used with a minimum threshold value of 95% for percent identity and 60% for percent coverage.

4.2.5 Detection of prophages in *K. pneumoniae* genomes (Laboratory isolates)

The web-based tool PHASTER, a bioinformatics resource portal available at http://phaster.ca/, was utilized to identify prophages and determine their completeness score in the genomes of *K. pneumoniae*. Additionally, the Proksee tool, accessible at https://proksee.ca/, was employed to visually display the circular genome and identify prophages in *K. pneumoniae* genomes.

4.2.6 Generation of a phylogenetic tree based on SNPs using WGS data

A phylogenetic tree was created using CSI Phylogeny 1.4 software, which was based on single nucleotide polymorphisms (SNP) for antimicrobial resistance. The software may be accessed at https://cge.food.dtu.dk/services/CSIPhylogeny/. The parameter specified a minimum depth of 10x at SNP positions, a minimum SNP quality of 30, a minimum relative depth of 10% at SNP positions, and a minimum Z-score of 1.96. The reference strain MGH 78578 (GenBank: CP000647.1) had been used for this analysis. Additionally, the tree data collected in Newick format was uploaded to the iTOL program (https://itol.embl.de/itol.cgi) for visualization purposes. The annotated and assembled data of STs, AMR genes and its location (on chromosome or plasmid), Plasmids, collection year, were then linked to the iTOL image.

4.2.7 Biofilm assay and categorization of Isolates

The biofilm formation of *K. pneumoniae* isolates (n = 27) was assessed utilizing the crystal violet method, and through the statistical analysis outlined by (Stepanović et al., 2007), the isolates were further classified as strong, moderate, and weak biofilm producers. In summary, LB (Luria Broth) and an overnight-grown culture (0.3 OD at 600 nm) were mixed in a 96-well microtiter plate, and the mixture was then incubated at 37 ^{0}C for 24 hours under static environments. The following day, the biofilm was subjected to a biofilm assay, which involved two rounds of washing with normal saline, 15 minutes of methanol fixation, and 15 minutes of 0.1% crystal violet (CV) staining. Subsequent to washing, the plates were permitted to dry in the air for 15 minutes. Following that, they were submerged in 33% glacial acetic acid and quantified using spectrophotometry at 570 nm. The isolates were classified into three categories: strong, moderate, and weak biofilm producers according to the cut-off optical density. The cut-off optical density (ODc) value was established at three standard deviations above the mean OD of the negative control group.The isolates were categorized as follows: weak biofilm producers (ODc <OD <

2ODc), moderate biofilm producers (2_ODc < OD < 4ODc), strong biofilm producers (4_ODc < OD), and no biofilm producer (OD ≤ ODc). Three replicates of each experiment were undertaken.

4.2.8 Isolate selection, Prophage Induction, and its effect on Biofilm formation

4.2.8.1 Isolate selection

Further, for the phenotypic experiment on prophage induction and its effect on biofilm, a total of eight isolates (M6, M10, M36, M52, M53, M55, M57, and DJ) were chosen. Among these, four isolates were identified as strong biofilm formers, three isolates were classified as moderate biofilm formers, and one isolate was found to be non-biofilm forming. These isolates except M10 and M36, were selected from the most abundant sequence types, ST231, and ST147.

4.2.8.2 Growth Curve for optimization of concentration of MMC of selected isolates

A growth curve experiment was conducted for all eight isolates using the synergy HT microplate reader (BioTek instruments, Winooski, VT, USA). A culture developed overnight (O.D. at 600 nm ~0.3) was introduced into 1 ml of fresh LB and thereafter incubated until the O.D. reached 0.05. Subsequently, 100 µL of culture (O.D. at 600 nm ~0.05) was transferred to a sterile 96-well flat-bottom microtiter plate, followed by the addition of different concentrations of MMC (0 µg/ml, 1 µg/ml, and 3 µg/ml) with only LB serving as the negative control and incubated at 37°C for 24 hours under continuous shaking conditions in an automatic microplate reader. The optical density (OD) at 600 nm was continually recorded at 15-minute intervals throughout a 24-hour period until the culture medium attained the stationary phase (Desai et al., 2019).

4.2.8.3 Prophage induction and biofilm assay

The prophage induction and biofilm formation were measured using the plaque assay and crystal violet assay. After the culture had grown overnight (O.D. at 600 nm = 0.1), 0µg/ml, 1µg/ml, and 3µg/ml MMC was included, and the combination was subjected to incubation at 37 °C for 24 hours. As a negative control, LB without bacterial culture was employed. Following a 24-hour period, a 100µl/ml chloroform treatment was administered, followed by ten minutes of inversion mixing and ten minutes of centrifuging at 10,000 rpm. The phage supernatant was collected. The supernatant of the chloroform-treated culture (Phage) was spotted on a host culture plate that had been preincubated, and the lawn was formed using a sterile swab stick and incubated for three to four hours and plaques were observed on next day shown in **Figure 4.1**. The Crystal violet

experiment was concurrently conducted to assess the impact of prophage induction via MMC on biofilm development, utilizing the method outlined in **section 4.2.7**.

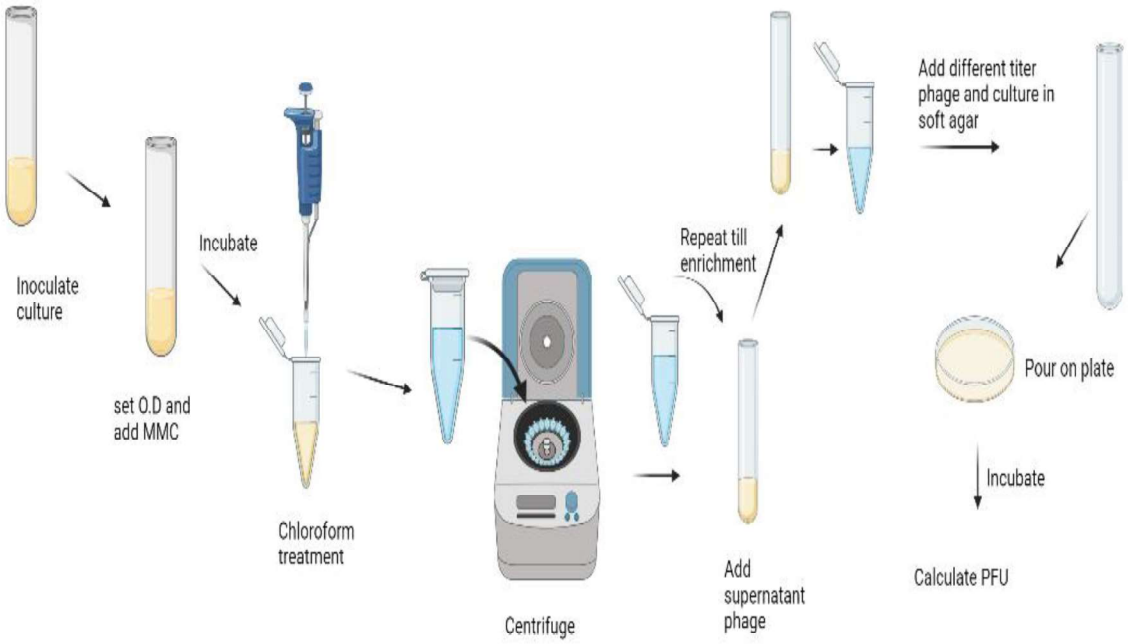

Figure 4.1 Diagrammatic representation of prophage induction. Overnight grown culture of *K. pneumoniae* with O.D. (0.1) at 600 nm was taken, the desired amounts of MMC {Mitomycin C serves as a typical drug for phage induction, inducing DNA damage and activating phages by stimulating the bacterial SOS response (Jancheva & Böttcher, 2021)} were added, and the mixture was kept at 37°C for 24 hours. It was then treated with chloroform, mixed inversionally for 10 minutes, and centrifuged at 10,000 rpm for 10 minutes. Then collected a supernatant potentially containing phages and applied it to 4 hours preincubated host plates, followed by overnight incubation and the presence of plaques (clear zones) was checked on the plates.

4.3 Results

4.3.1 Meta-data of retrieved genomes

Genome retrieved for isolates collected from various regions of India are shown in **Figure 4.2**. Most of the isolates (n = 128, 61.24%) were from Tamil Nadu, followed by Gujarat (n = 22, 10.52%), West Bengal (n = 21, 10.04%), New Delhi (n = 11, 5.26%), and Assam (n = 10, 4.78%). Less than 2% of the isolates were detected from Kerala, Maharashtra, Madhya Pradesh, Uttar Pradesh, Punjab, and Odisha. Whereas the geographic location of isolate 1 was not specified.

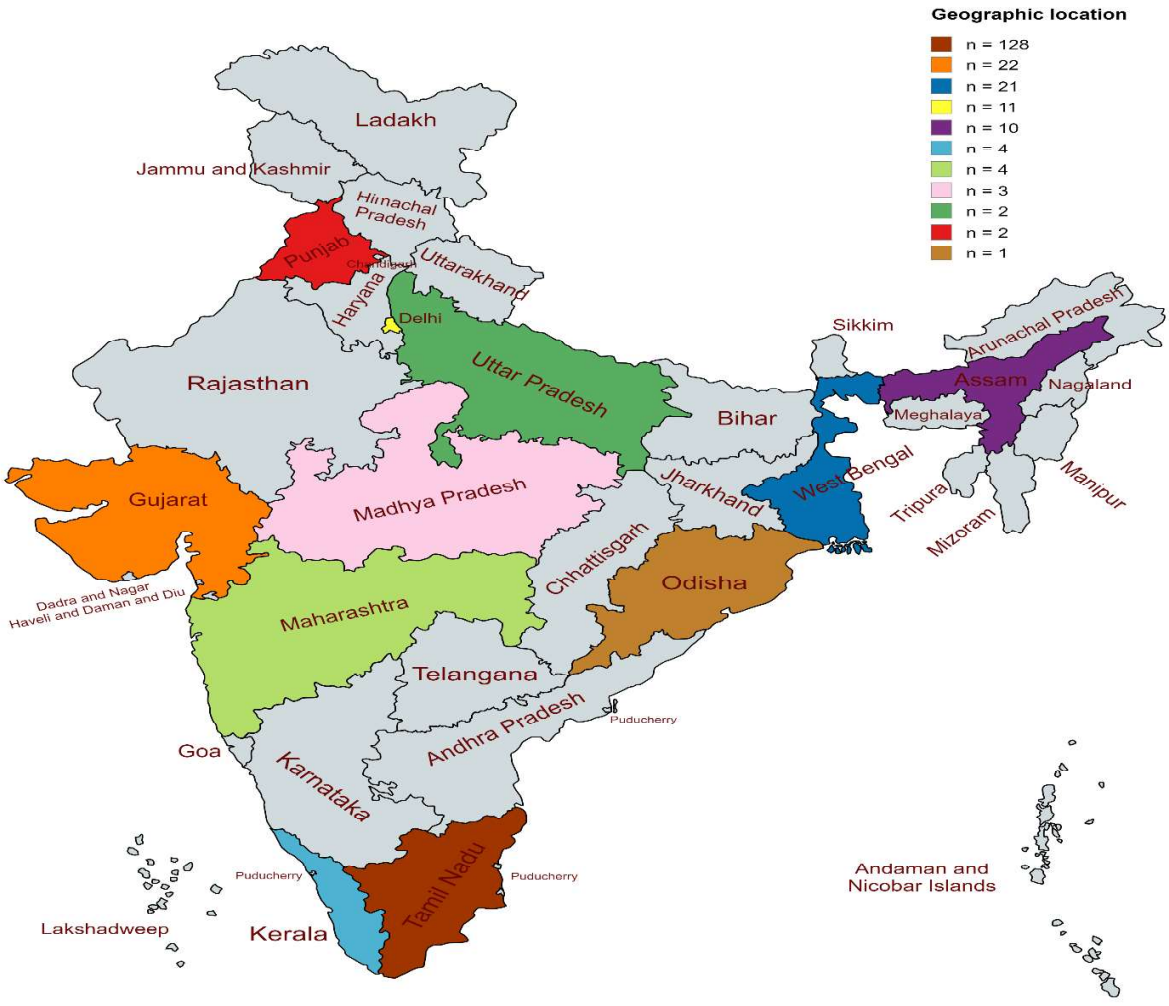

Figure 4.2 Distribution of whole genome sequenced isolates from several states in India. Most of the isolates were from southern India, mainly from Tamil Nadu and a small number from Kerala. The north-eastern states of West Bengal and Assam, as well as the western states of Gujarat and Maharashtra, followed this.

Furthermore, the isolates were grouped according to the host's source of isolation. The majority of the specimens, or 49.28% of the cases, had bloodstream infections. Respiratory tract infections came next, accounting for 27.75%, followed by urinary tract infections at 8.61%. The prevalence of isolates from other infection sites, such as nosocomial, sepsis, wound, CNS, and implant artificial, was less than 1%. However, approximately 11.48% of isolates did not have any available infection sites in the metadata as shown in **Figure 4.3.**

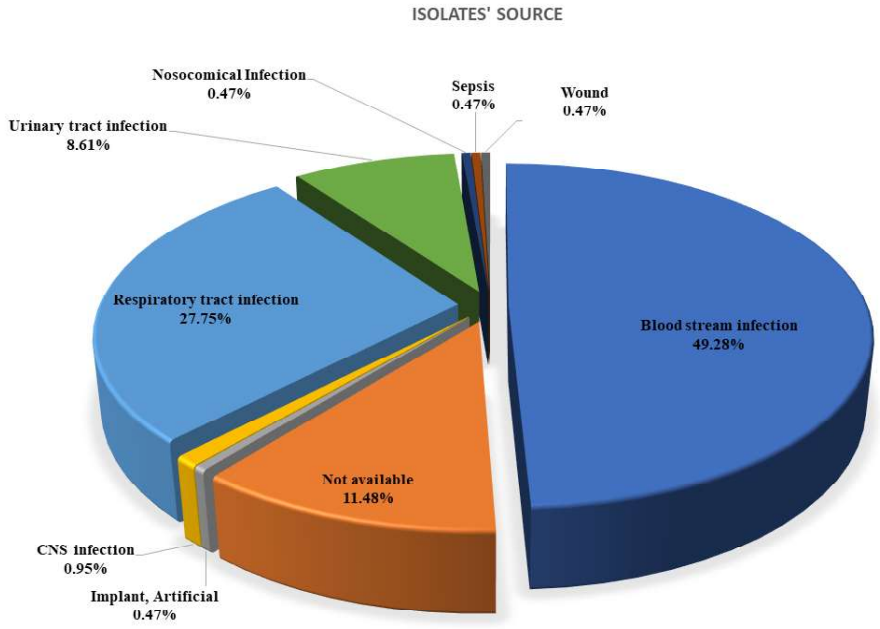

Figure 4.3 Segmentation of isolates according to the place of infection or source of isolation. The bulk of isolates came from cases of blood stream infections, then respiratory tract infections and urinary tract infections. However, others were occasionally.

Subsequently, the isolates were further organized according to their sample origin, distinguishing between human, environmental, or other sources. Out of the total isolates, 92.28% were from human origin, 6.69% were from environmental sources, and only one isolate did not have information on its sample type, as depicted in the **Figure 4.4.**

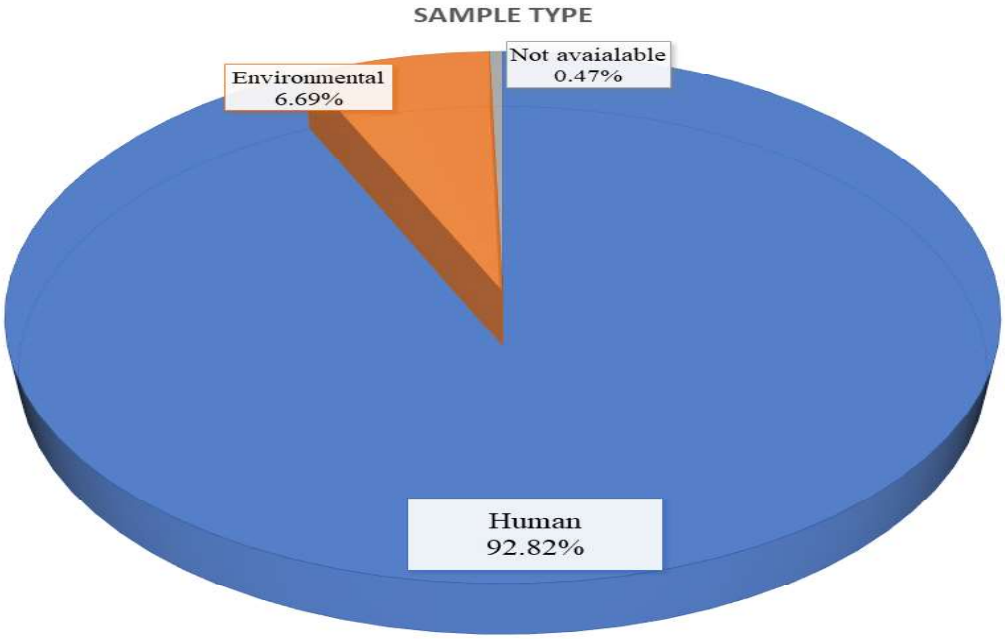

Figure 4.4 Shows the distribution of sample types. More than 92% of the isolates were derived from human sources, with environmental sources and unknown sample types being less common.

4.3.2 Multi-locus sequence typing of isolates

4.3.2.1 Sequence type determination of lab isolates (n = 29)

In order to identify the sequence types, the allelic combinations of 7 housekeeping genes were identified and compared to known sequence types using an in-silico approach. A total of 18 distinct sequence types were identified as shown in **Table 4.1**, with ST231 being the most common, followed by ST147 and ST2096. Also, two new alleles, 764 and 765 of the *tonB* gene, were found in isolates M10 and M33, respectively. Therefore, the PasteurMLST database designated 2 new sequence types (STs) 5438 and 5439 based on these unique combinations of alleles as highlighted with green colour in **Table 4.1**. Isolate M27 exhibits a potential new allele for the *tonB* gene and may represent a previously unidentified sequencing type. Regrettably, the analysis could not include the data since it exceeded the threshold of 500 contigs, which is the qualification criteria for the PasteurMLST database.

Table 4.1 Illustrates the dispersion of alleles and sequence type in lab isolates (*n* = 29)

Isolates	*gapA*	*infB*	*mdh*	*pgi*	*phoE*	*rpoB*	*tonB*	Sequence type
M2	2	6	1	3	26	1	77	231
M6	2	6	1	3	26	1	77	231
M10	198	1	2	1	10	4	**764**	**5438**
M17B	1	6	1	1	1	1	1	14
M25	2	1	1	1	3	3	38	1087
M27	198	52	2	1	12	1	-	**~2943**
M33	198	1	2	1	7	152	**765**	**5439**
M34a	2	1	1	3	8	25	15	1715
M35	2	1	169	12	9	4	40	3020
M36	2	9	2	1	13	1	16	37
M39	3	4	6	1	7	4	4	273
M40	2	1	2	1	10	4	46	280
M44	2	6	1	5	363	1	708	5217
M46	2	1	1	6	7	1	12	45
M47	2	6	1	3	26	1	77	231
M48	1	6	1	1	1	46	1	2096
M49	3	4	6	1	7	4	38	147
M50	2	6	1	3	26	1	77	231
M51	2	6	1	3	26	46	77	5785
M52	2	6	1	3	26	1	77	231
M53	3	4	6	1	7	4	38	147
M54	2	1	2	1	4	4	4	16
M55	3	4	6	1	7	4	38	147
M56	1	1	1	1	1	1	1	15
M57	2	6	1	3	26	1	77	231
M58	3	3	1	1	1	1	4	11
M59	2	6	1	3	8	1	15	42
DJ	3	4	6	1	7	4	38	147
ST1	1	6	1	1	1	46	1	2096

4.3.2.2 Sequence type determination of Pan-India K. pneumoniae isolates (n = 209)

In this study, we identified 50 distinct sequence types that were present in India *K. pneumoniae* genomes which also includes genome of the lab isolates. Among these, ST231 was the most widespread, accounting for 33.49% (n = 70) of the samples. ST147, ST2096, and ST14 were also prevalent, representing 10.04% (n = 21), 7.17% (n = 15), and 5.74% (n = 12) of the samples, respectively as shown in figure 4.4. Additional sequence types (STs), including ST11, ST15, ST16, ST23, ST35, ST42, ST43, ST48, ST101, ST307, ST395, ST420, ST437, and ST515 were associated with a minimum of 2 genomes. Furthermore, a total of 32 distinct STs were detected in individual genomes as shown in **Figure 4.5.**

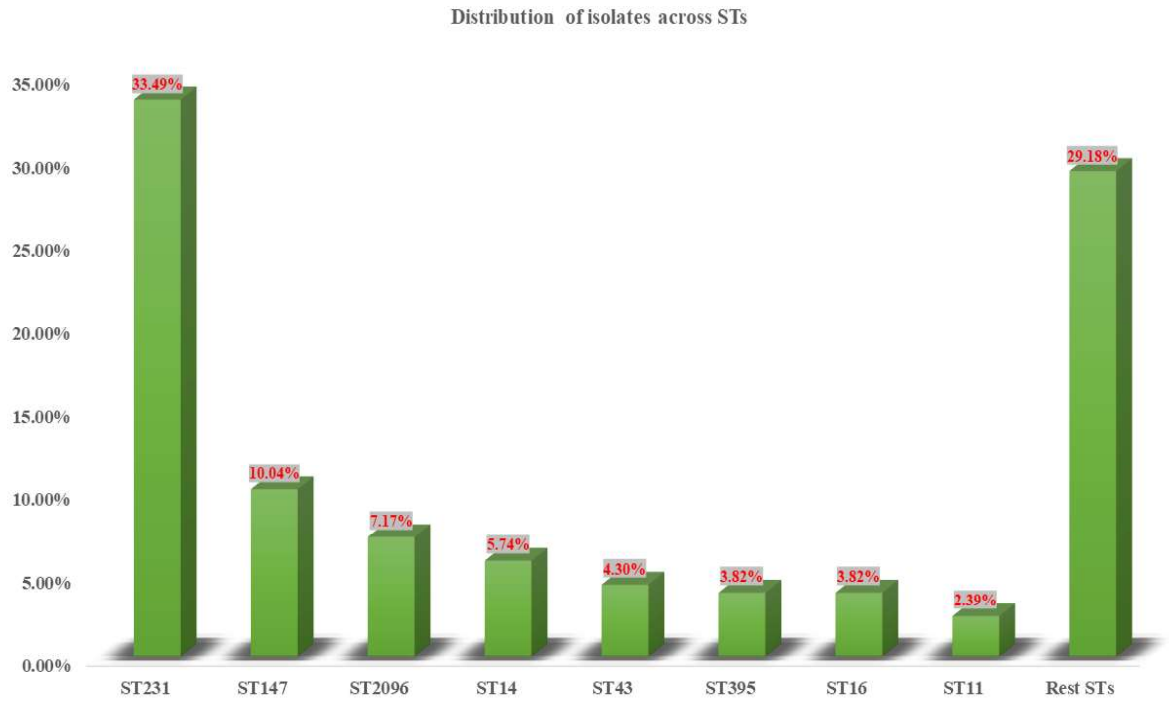

Figure 4. 5 Distribution of isolates among different sequence types identified in India. Several isolates, consisting of a minimum of five, were presented here, while the remaining ones were labeled as Rest STs.

4.3.2.3 The geographic distribution of Sequence Types in various regions of India

We identified ST231 as the predominant ST throughout the entire India. ST147 was detected in Tamil Nadu, West Bengal, Gujarat, and Uttar Pradesh, whereas ST2096, ST16, and ST42 were observed in Tamil Nadu and Gujarat. ST14 was identified in Tamil Nadu, Gujarat, West Bengal,

and New Delhi, but ST307 was exclusively found in Assam. The distribution of Sequence types (STs) each state is illustrated in **Figure 4.6.**

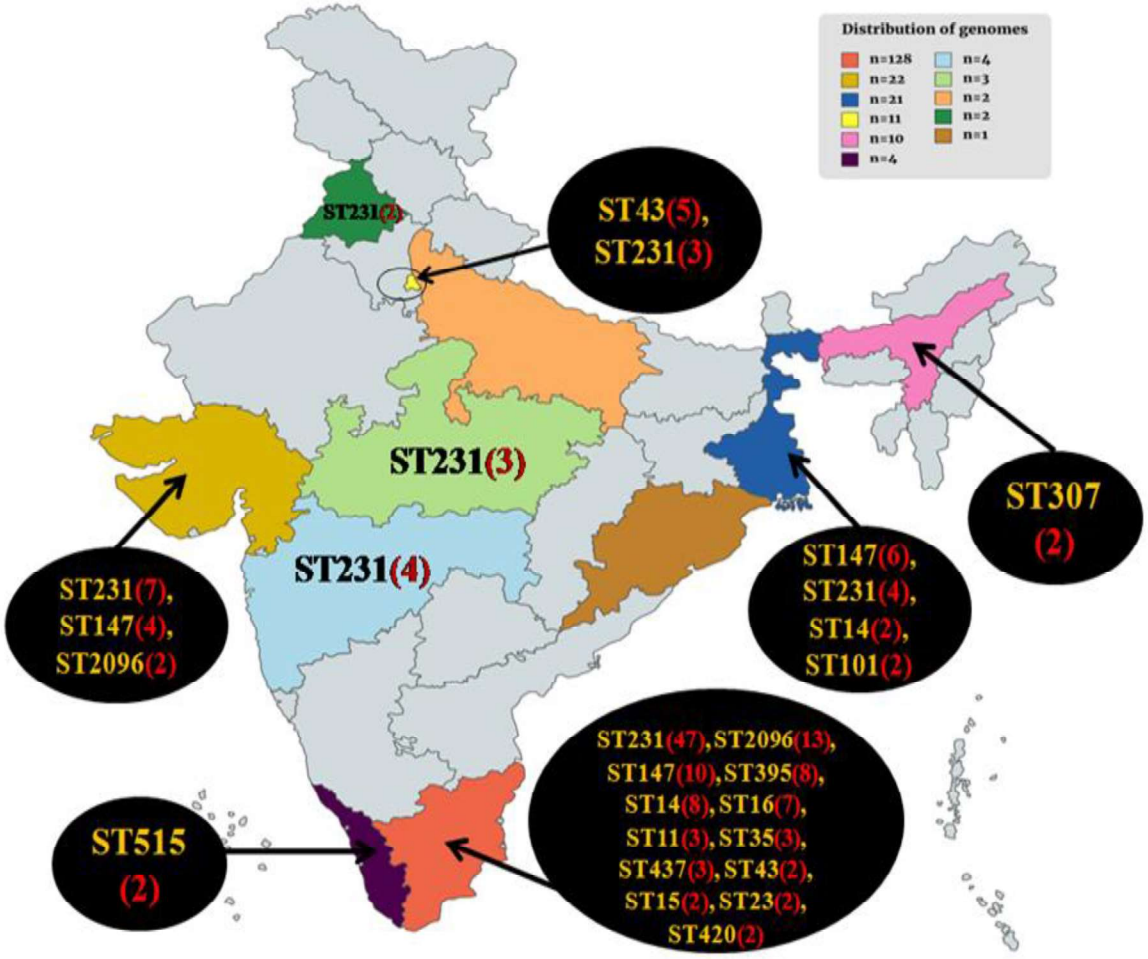

Figure 4.6 The geographical distribution of the genome collection and the distribution of sequence types in India. This figure includes STs that are present in at least 2 genomes. The number of genomes is shown, with each state being assigned a certain color. The variable (n) represents the quantity of genomes, while the colors symbolize the different states. The ST231 strain was prevalent among isolates and found in almost all states of India, with the exception of Assam denoted in Pink colour. The states are represented by specific colors: Tamil Nadu is depicted by carrot red, Gujarat by mustard yellow, West Bengal by cyan, New Delhi by yellow, Assam by pink, Kerala by purple, Maharashtra by sky blue, Madhya Pradesh by pastel green, Uttar Pradesh by orange, Punjab by green, and Odisha by brown.

4.3.3 Detection and distribution of beta-lactamase genes among isolates.

The identification of antibiotic resistance genes, specifically those responsible for beta-lactam antibiotics, was conducted across isolates. Furthermore, the beta-lactamase genes were categorized into four groups according to their functional characteristics as documented in the Beta-Lactamase Database (http://bldb.eu/). Four distinct categories of β-lactamase genes, including carbapenemases, extended spectrum beta-lactamases, broad spectrum beta-lactamases,

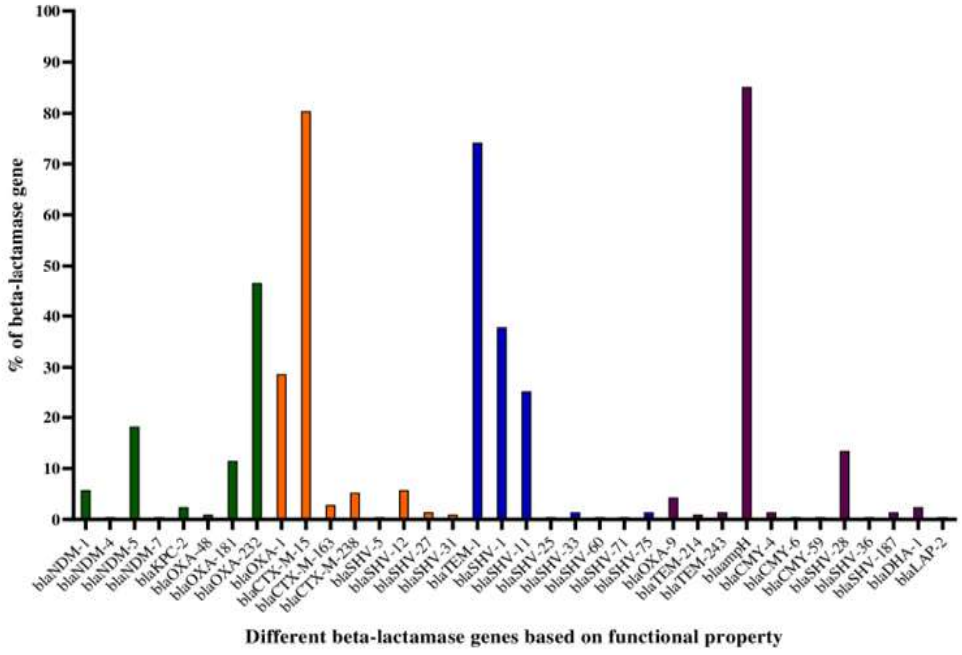

Figure 4.7 Proportionate allocation of β-lactamase genes among different strains. The bars in the graph denote distinct β-lactamase genes. The green bars show the presence of the carbapenemase gene, the orange bars indicate the presence of ESBLs, the blue bars indicate the presence of BSBLs, and the purple bars indicate the presence of additional β-lactamase genes. This graph was generated using the GraphPad Prism 8.4.2 software.

and additional beta-lactamase genes, were identified in *K. pneumoniae* genomes. A total of 36 distinct beta-lactamase genes were identified across genomes as shown in **Figure 4.7**. Among these, there were a total of 8 carbapenemase genes, with *bla*OXA-231 and *bla*NDM-5 being the most found. Additionally, there were 8 extended spectrum beta-lactamases, with *bla*CTX-M-15 and *bla*OXA-1 being the most prevalent. Lastly, there were 8 broad spectrum beta-lactamases, with *bla*TEM-1, *bla*SHV-1, and *bla*SHV-11 being the most frequently observed. In addition, a total of 12 distinct variants of beta-lactamases were identified, with *bla*ampH and *bla*SHV-28 being the most widespread.

4.3.3.1 The location and distribution of beta-lactamase genes within STs.

4.3.3.1.1 Distribution of Carbapenemases

The distribution of carbapenemase genes was found to change among distinct sequence types (STs) as shown in **Figure 4.8** and **Figure 4.9**. The carbapenemase genes, specifically *bla*OXA-48-like (including *bla*OXA-48, *bla*OXA-232, and *bla*OXA-181), were identified as the most commonly found among Indian isolates. Among these, *bla*OXA-232 was the most abundant carbapenemase, detected in 46.41% (n = 97) of the overall genomes. The *bla*OXA-232 gene was predominantly found in genomes belonging to the ST231 lineage, accounting for 61.85% (n = 60) of the cases. In addition to ST231, the genomes of ST2096 (12.37%, n = 12) and ST14 (8.24%, n = 8) also included the *bla*OXA-232 gene. The other 18% of *bla*OXA-232 genes were found in the genomes of ST23, ST147, ST437, and ST395. Four different forms of *bla*NDM were identified, specifically, *bla*NDM-1, *bla*NDM-4, *bla*NDM-5, and *bla*NDM-7. Out of these, *bla*NDM-5 was found to be the most common (18.18%, n = 38), followed by *bla*NDM-1 (5.74%, n = 12). The *bla*NDM-4 and *bla*NDM-7 genes were each detected in only one isolate, which belonged to ST11 and ST711, respectively. Out of the *bla*NDM-5 samples analyzed, 28.94% (n = 11) were determined to be carried by ST147, which is one of the commonly occurring STs in India. In addition, *bla*NDM-5 was identified in other clinically less common sequence types (STs): ST395, ST437, ST16, ST14, and ST101. The *bla*NDM-1 gene was primarily identified in strains belonging to sequence types 14 (ST14) and 11 (ST11). Individual strains of ST147, ST231, ST273, ST624, and ST2816 were also found to possess the *bla*NDM-1 gene. However, just one strain of ST231 was confirmed to have a *bla*NDM variation, specifically *bla*NDM-1. The *bla*KPC-2 gene was detected in just four genomes of ST147 and one genome of ST101. *bla*NDM and *bla*KPC were less frequent in India compared to *bla*OXA-232. The *bla*OXA-181 gene was predominantly detected in ST43, ST147,

and ST16, accounting for 11.48% of the samples (*n* = 24). The *bla*OXA-48 gene was detected in just two genomes belonging to the ST101 lineage. A few genomes were found to contain five distinct combinations of dual carabapenemase genes. The presence of *bla*NDM-5 + *bla*OXA-232 was identified in ST147 (*n* = 4), ST437 (*n* = 3), ST2096 (*n* = 2), ST395 (*n* = 2), and ST14 (*n* = 1). The combination of *bla*NDM-5 + *bla*OXA-181 was detected in ST16 (*n* = 5) and ST147 (*n* = 4). The occurrence of *bla*NDM-5 + *bla*OXA-48 was observed in ST101 (*n* = 2). The presence of *bla*NDM-1 + *bla*OXA-232 was detected in ST14 (*n* = 3). Lastly, *bla*NDM-1 + *bla*OXA-181 was found in ST14 (*n* = 1), ST11 (*n* = 1), and ST42 (*n* = 1).

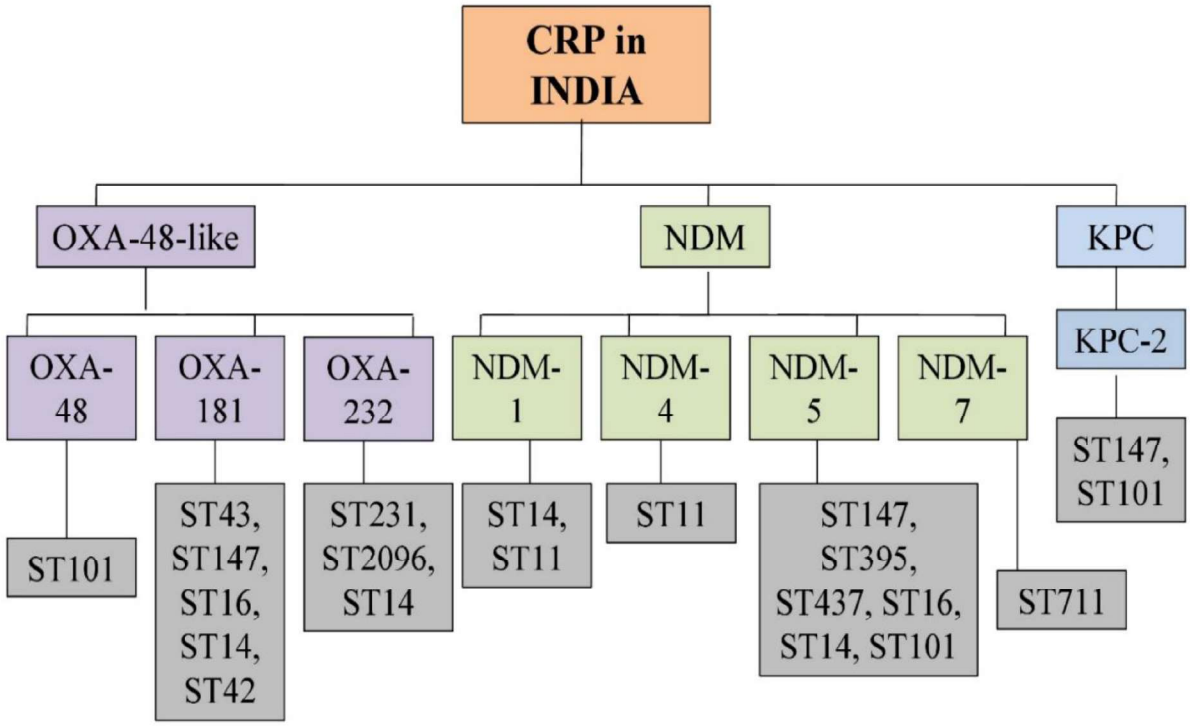

Figure 4.8 Distribution of carbapenemase genes circulating in India. This chart illustrates the incidence of three significant carbapenemase genes: *bla*OXA-48 like, *bla*NDM, and *bla*KPC, along with their correlation with certain sequence types.

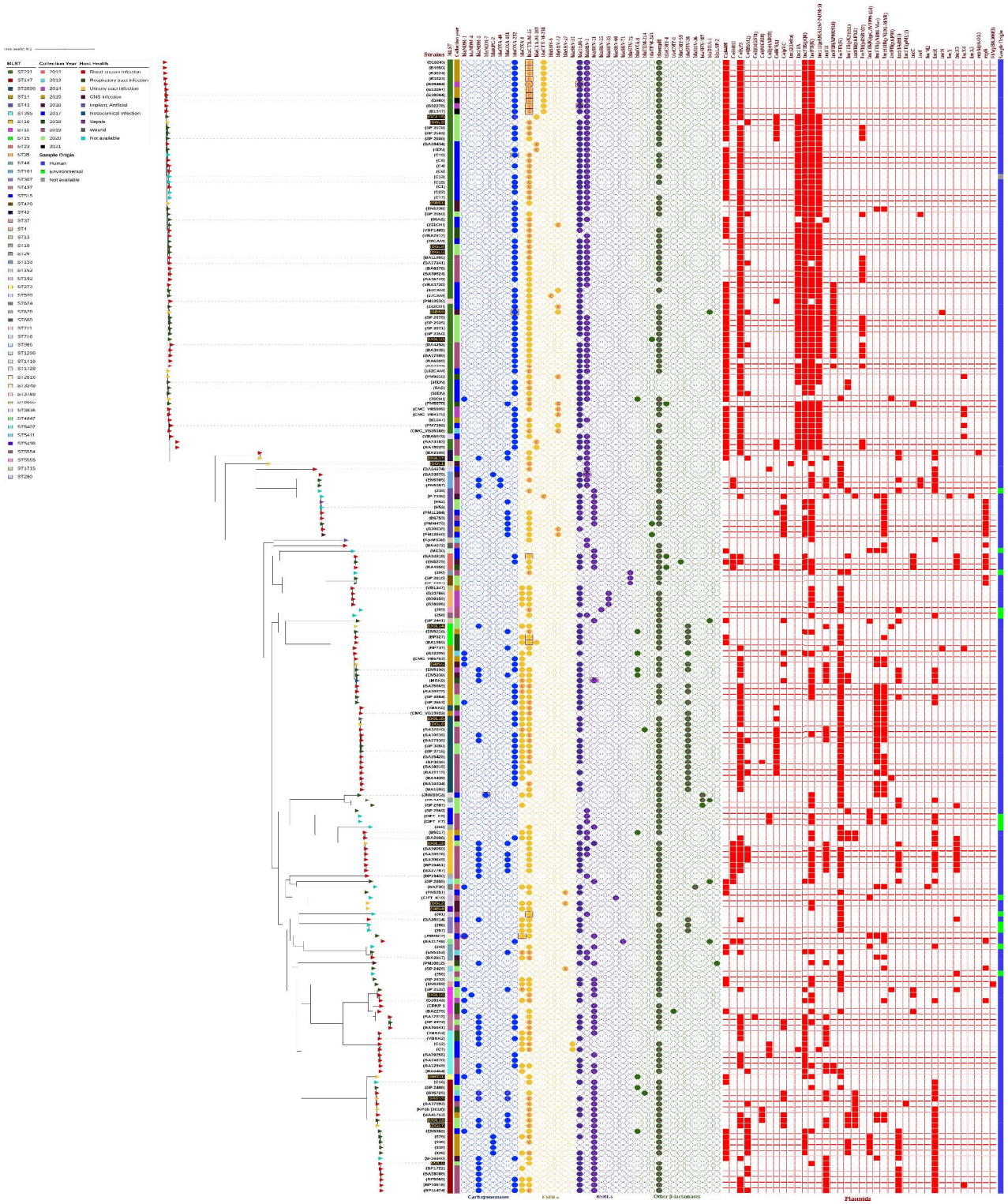

Figure 4.9 *β*-lactamases and the plasmid replicons present in *K. pneumoniae* genomes from India. The yellow strains represent the laboratory isolates, whereas the black strains represent the recovered genomes. The presence of beta-lactamase genes is shown by circles filled with different colors: blue for carbapenemase, yellow for ESBLs, purple for BSBLs, and green for other β-lactamases. Circles that are not filled indicate the lack of these genes. The presence of the letter C within a circle signifies that the genes are situated on a chromosome, whereas its absence denotes that the gene resides on a plasmid. A red ring around the circle signifies the existence of three gene copies. A dark red square surrounding the circle signifies the presence of two gene copies. The letters C and P signify that one copy of the gene is on a chromosome while the other copy is situated on a plasmid. Plasmids are represented by a red filled square to indicate their existence, whereas an empty square indicates their absence. The picture was generated using iTOL.

In terms of the placement of carbapenemase genes, it was found that all *bla*OXA-232 genes were situated on plasmids, with the exception of two genomes (DGL15, and EN5338). The presence of two instances of the *bla*OXA-232 gene was identified in two genomes, specifically C18 and SBS3. *bla*OXA-181 was found on the chromosome in two genomes (B35725 and SBS12), while the remaining genomes had it on plasmids. All *bla*NDM-5 genes were identified on plasmids in all genomes excluding two genomes, B35725 and SBS12. There were few genomes contained plasmids carrying both *bla*OXA-48 and *bla*KPC. The presence of *bla*NDM-1 was seen exclusively on plasmids, with the exception of one genome (JNM8C2) which contained three copies of *bla*NDM-1 on the plasmid.

4.3.3.1.2 Distribution of Extended-Spectrum β-Lactamases

The *bla*CTX-M-15 was the most prevalent, accounting for 80.38% (n = 168) of the total ESBLs. *bla*CTX-M-15 was present in the genomes of the majority of ST231, ST147, ST2096, ST11, ST14, ST15, ST16, ST23, ST43, ST45, ST48, ST307, ST395, and ST437. Only the less common sequence types (STs) such as ST515, ST420, and ST101 did not possess the *bla*CTX-M-15 gene. The *bla*CTX-M-15 gene was identified on both chromosomes and plasmids. The *bla*CTX-M-15 gene was found on plasmids in ST16 genomes, but in ST231 (n = 9), two copies of the *bla*CTX-M-15 gene were found on the chromosomes. In addition, a single genome B28484 that belonged to ST231 contained three copies of *bla*CTX-M-15, which were situated on the chromosome. Four genomes, namely belonging to ST15, ST23, and ST152, were found to carry a duplicated copy of the *bla*CTX-M-15 gene on their plasmids. The presence of both *bla*CTX-M-15 and *bla*OXA-232 was detected in 39.7% (n = 83) of the genomes. The genomes of ST231 (77.14%, n = 54/70), ST2096 (66.66%, n = 10/15), ST14 (50%, n = 6/12), ST437 (100%, n = 3/3), and ST23 (66.66%, n = 2/3) showed the simultaneous presence of *bla*CTX-M-15 and *bla*OXA-232. In addition to *bla*CTX-M-15, another Extended-Spectrum Beta-Lactamase (ESBL), *bla*OXA-1 (28.70%, n = 60), was also identified as the most common in the genomes. The *bla*OXA-1 gene was not found in the genomes of the most common ST231 strain. However, it was most commonly detected in the ST2096 strain (21.66%, n = 13), followed by ST14 (18.33%, n = 11), ST147 (10%, n = 6), and ST395 (10%, n = 6). *bla*OXA-1 was identified in a limited number of genomes belonging to other common sequence types, including ST16, ST11, ST15, ST35, ST48, and ST307. The *bla*OXA-1 gene was found on the chromosome in one genome each of ST2096, ST48, and ST11, as well as in three genomes of ST14. In the remaining genomes, the gene was located on plasmids among different STs.

4.3.3.1.3 Distribution of Broad-Spectrum β-Lactamases

The most commonly detected broad-spectrum β-lactamase (BSBL) was *bla*TEM-1, accounting for 74.16% (*n* = 155) of the cases. Among the different sequence types, ST231 had the highest prevalence at 42.58% (*n* = 66), followed by ST147 at 9.03% (*n* = 14), ST2096 at 7.74% (*n* = 12), ST14 at 5.80% (*n* = 9), ST16 at 4.51% (*n* = 7), ST43 at 3.87% (*n* = 6), and ST395 at 3.22% (*n* = 5). Among various sequence types, 41.14% (*n* = 86) of genomes were discovered to have both *bla*OXA-232 and *bla*TEM-1, whereas 65.55% (*n* = 137) of genomes had both *bla*CTX-M-15 and *bla*TEM-1. The presence of these three genes (carbapenemase—*bla*OXA-232, ESBLs—*bla*CTX-M-15, and BSBLs—*bla*TEM-1) was found to co-occur in 37.79% (*n* = 79) of the genomes. The presence of *bla*TEM-1 genes was observed on plasmids in all genomes, except for two genomes each of ST231 and ST43. In addition to *bla*TEM-1, two other broad-spectrum beta-lactamases, namely *bla*SHV-1 (37.79%, *n* = 79) and *bla*SHV-11 (25.35%, *n* = 53), were identified as the most prevalent among the genomes studied. The *bla*SHV-1 gene was predominantly found in the genomes of ST231 (72.15%, *n* = 57), followed by ST16 (5.06%, *n* = 4), ST101 (3.79%, *n* = 3), ST515 (3.79%, *n* = 3), and ST48 (2.53%, *n* = 2).

Surprisingly, we could not detect any *bla*SHV-1 in the genomes of other commonly found sequence types including ST147, ST2096, ST14, ST43, ST395, ST11, ST15, ST23, ST35, ST307, and ST437. All the genes of *bla*SHV-1 were identified on chromosomes, except for one genome (BA39950) of ST16 and one genome (BA33875) of ST101, which were found to have two copies of this gene. In these cases, one copy was situated on the chromosome while the second copy was found on the plasmid. The *bla*SHV-11 gene was predominantly found in the ST147 strain (39.62%, *n* = 21), followed by ST43 (13.20%, *n* = 7) and ST395 (7.54%, *n* = 4). In addition, several additional common sequence types, including ST11, ST23, and ST437, were found to have the *bla*SHV-11 gene in their genetic makeup. It is worth noting that the most widespread ST231, along with ST2096, ST14, and ST16, did not possess the *bla*SHV-11 gene, save for one instance each in the genomes of ST14 and ST16. The gene *bla*SHV-11 was identified on many chromosomes, except for DGL12 (ST16). However, the strain MRK9 was found to have two copies of *bla*SHV-11. One copy was situated on the chromosome, while the second copy was detected on the plasmid.

4.3.3.1.4 Distribution of other β-Lactamases

In addition to the frequently seen carbapenemases, ESBLs, and BSBLs, other β-lactamases, such as *bla*ampH, which is a penicillin-binding protein related to AmpC, were discovered to be most prevalent (85.16%, n = 176) throughout genomes. Furthermore, all *bla*ampH genes were identified on chromosomes. The *bla*SHV-28 gene was found in ST2096, ST14, ST15, and ST307, with a prevalence of 13.39% (n = 28). All *bla*SHV-28 genes were found on chromosomes, with the exception of one genome (B32205) belonging to ST14. Several variants of *bla*SHV (including *bla*SHV-5, *bla*SHV-12, *bla*SHV-25, *bla*SHV-27, *bla*SHV-31, *bla*SHV-33, *bla*SHV-36, *bla*SHV-60, *bla*SHV-71, *bla*SHV-75, *bla*SHV-187), *bla*CTX-M (such as *bla*CTX-M-163, *bla*CTX-M-238), *bla*TEM (such as *bla*TEM-214, *bla*TEM-243), and *bla*CMY (including *bla*CMY-4, *bla*CMY-6, *bla*CMY-59), as well as *bla*OXA-9, *bla*DHA-1, and *bla*LAP-2, were identified in a small number of genomes.

4.3.4 Distribution of plasmid replicons among dominant sequence types

Indian genomes were found to have a wide range of plasmid combinations, and various plasmid combinations were observed to be linked to specific STs (**Figure 4.9** and **Figure 4.10**). For example, the majority of ST231 genomes included Col440I and ColKP3, whereas only a small number of ST231 genomes carried ColRNAI. ColRNAI was primarily linked to ST2096 and ST23. ST14 and ST2096 primarily harbored ColKP3. The Col(BS512) plasmid was found in a high abundance in genomes belonging to the ST147 strain, but was not commonly found in the ST231, ST14, and ST2096 strains. ColpVC was observed to have a strong association with ST43, but only a weak association with ST147 and ST437. Col440II was found in the ST16, ST23, and ST101 strains, which are commonly present. IncF plasmids were found to be linked with variety of sequence types (STs). ST231 genomes exhibited a high abundance of IncFIA, IncFIB(pQil), IncFII(K), and IncF(pAMA1167-NDM-5). On the other hand, ST14 genomes only included IncFII(K) and IncFIB(K), which were not found in ST231 genomes. Several sequence types (STs), namely ST395, ST147, ST43, and ST11, were discovered to have a connection with IncFIB(pQil). The IncHI1B(pNDM-MAR) plasmid was predominantly harbored by the ST2096, ST14, and ST43 strains. The genomes of ST147, ST395, ST14, and ST16 included the IncFII genetic element. The IncFIB(pNDM-Mar) plasmid was primarily found in the ST2096 and ST14 sequence types. The presence of IncR was found to have a substantial correlation with ST147, whereas genomes of ST147 also showed the presence of IncFIB(pKPHS1), IncFII(pKPX1), and ColpVC.

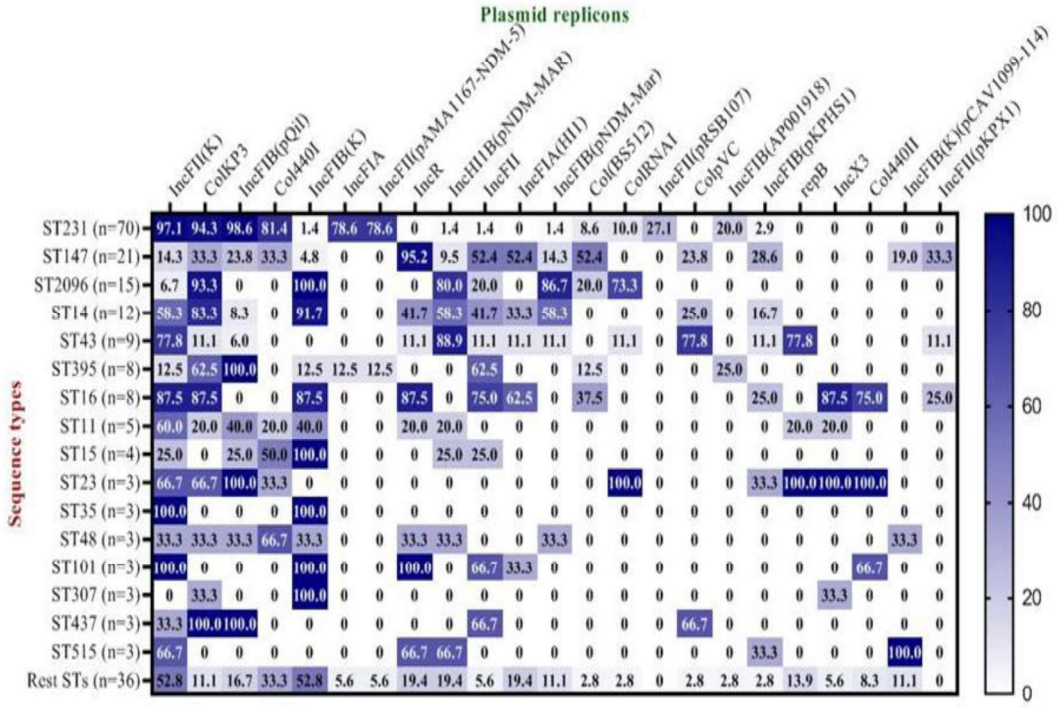

Figure 4.10 Heatmap illustrating the percentage distribution of plasmid replicons among different sequence types (STs). (n) Represents the aggregate quantity of specific STs. The scale represents 100% with dark blue and 0% with white. This heatmap was generated using the GraphPad Prism 8.4.2 software.

4.3.5 Investigation of the genotypic and phenotypic connection of Carbapenem resistance in selected isolates.

The primary factor contributing to carbapenem resistance in *K. pneumoniae* is the presence of carbapenemase genes, including *bla*OXA-48-like, *bla*NDM, and *bla*KPC types. However, other variables like as efflux pumps and the loss or mutations in porins also contribute to the increased resistance to carbapenem drugs (Reyes, 2005; Shahid et al., 2022). Nevertheless, in this investigation, we discovered some isolates that had dual carabapenemase genese *bla*OXA-48-like and *bla*NDM type. Furthermore, we deliberately chose these isolates, along with those that had only one or no carbapenemase genes, to investigate if the presence of dual

carbapenemase genes may increase the level of minimum inhibitory concentration (MIC) in *K. pneumoniae*.

4.3.5.1 Carbapenemase genes

Isolate M40 did not have the carbapenemase gene. However, isolate M52 had the *bla*OXA-232 carbapenemase gene, isolate M39 had the *bla*NDM-1 carbapenemase gene, an extra isolate from lab J20 was deliberately incorporated to represent the blaOXA-181 carbapenemase gene, and isolate M53 had the *bla*NDM-5 carbapenemase gene. Dual carbapenemase was found in M49 and M17B, which included *bla*NDM-5 + *bla*OXA-181 and *bla*NDM-1 + *bla*OXA-232, respectively as mentioned in **Table 4.2.**

Table 4.1 List of known carbapenemase genes, mutations, or loss of porins, and efflux pumps related to carbapenem resistance.

Isolates	*Carbapenemase genes*	*Loss or mutations of Porins*			*Efflux pumps*
		ompK35	*ompK36*	*ompK37*	
M40	*None*	*None*	*p.A217S*	*p.I70M, p.I128M, m233_None234insQ*	*KpnG, KpnH, LptD, marA*
M52	*blaOXA-232*	*None*	*Gene not found (Loss of Porin)*	*p.I70M, p.I128M, p.N230G, m233_None234insQ*	*KpnG, KpnH, LptD, marA*
M39	*blaNDM-1*	*None*	*p.A217S*	*None*	*KpnG, marA*
J20	*blaOXA-181*	*None*	*p.A217S*	*p.I70M, p.I128M*	*KpnG, KpnH, marA*
M53	*blaNDM-5*	*None*	*p.A217S*	*p.I70M, p.I128M*	*KpnG, KpnH, marA*
M49	*blaNDM-5, blaOXA-181*	*None*	*p.A217S*	*p.I70M, p.I128M*	*KpnG, KpnH, LptD, marA*
M17B	*blaNDM-1, blaOXA-232*	*None*	*p.A217S, p.N218H*	*p.I70M, p.I128M*	*KpnG, KpnH, marA*

4.3.5.2 Loss or Mutations of Porins

This study focused on the examination of three specific porins, namely ompK35, ompK36, and ompK37, in order to identify any instances of porin loss or porin alterations. None of the seven isolates showed the presence of the well-documented mutation, ompK35, which is associated

with carbapenem resistance. All isolates with ompK36, except M52, were found to have a single mutation in the amino acid p.A217S. However, in the case of M52, a deletion of this porin was discovered. A specific mutation, p.N218H, was found exclusively in M17B, in addition to other mutations in the *ompK* gene. Significant alterations were identified in the *ompK37* gene, indicating resistance to carbapenem drugs. All isolates, save M39, were found to have dual mutations p.I70M and p.I128M. Both M40 and M52 exhibited the presence of an extra mutation, specifically m233_None234insQ. However, the mutation p.N230G was only discovered in M52 (**Table 4.2**). However, the investigation could not find any isolate that had the combination of *bla*NDM-5 + *bla*OXA-232, as well as *bla*NDM-1 + *bla*OXA-181. Consequently, the study was unable to examine the impact of this combination on the minimum inhibitory concentration.

4.3.5.3 Efflux pumps

Four efflux pumps associated with carbapenem resistance were identified in the isolates. These pumps are *KpnG, KpnH*, *LptD,* and *marA*, all of which were recognized in M40, M49, and M52. M17B and M39 both exhibited the presence of *KpnG* and *marA*. In addition, *KpnH* was found in J20, M17B, and M53. The genes *KpnG* and *marA* were identified as the most prevalent, being present in all isolates. All porin modifications, except for p.N230G found in M52, were identified as common between the carbapenemase negative (M40) and the carbapenememase positive isolates (M17B, M39, M53, M49, and J20). There was no variation in the presence of efflux pumps across the seven isolates.

4.3.5.4 Analysis of the phenotypic characteristics associated with resistance to carbapenem

Ertapenem and meropenem, which are classified as group 1 and group 2 carbapenem drugs respectively, were utilized to determine the minimum inhibitory concentration. Isolate M40 was chosen as the negative control isolate for the carbapenemase gene, with lower MIC values of 8 µg/mL for ertapenem and 1 µg/mL for meropenem. While the remaining isolates (M17B, M39, M49, M52, M53, and J20) were resistant to both ertapenem and meropenem, the MIC values for ertapenem were significantly higher compared to meropenem. The MIC values for different strains of bacteria yielding single carbapenemase were as follows: M52 (*bla*OXA-232) had a MIC of 128 µg/mL for ertapenem, M39 (*bla*NDM-1) had a MIC of 16 µg/mL for ertapenem, J20 (*bla*OXA-181) had a MIC of >512 µg/mL for ertapenem, and M53 (*bla*NDM-5) had a MIC of >512 µg/mL for ertapenem. For meropenem, the MIC values were 64 µg/mL for M52, 4 µg/mL for M39, 128 µg/mL for J20, and 512 µg/mL for M53. Finally, the minimum inhibitory concentration values of the dual carbapenemase producers, M17B (with *bla*OXA-

232 and *bla*NDM-1 genes) and M49 (with *bla*OXA-181 and *bla*NDM-5 genes), were shown to be 128 µg/mL for ertapenem and >512 µg/mL for meropenem (figure 4.11). It was found that isolates with a single carbapenemase (*bla*OXA-181 or *bla*NDM-5) type or a dual carbapenemase (*bla*OXA-181 + *bla*NDM-5) type were more resistant to both antibiotics than the isolates with a single carbapenemase (*bla*OXA-232 and *bla*NDM-1) type or a dual carbapenemase (*bla*OXA-232 + *bla*NDM-1) type. This finding is intriguing.

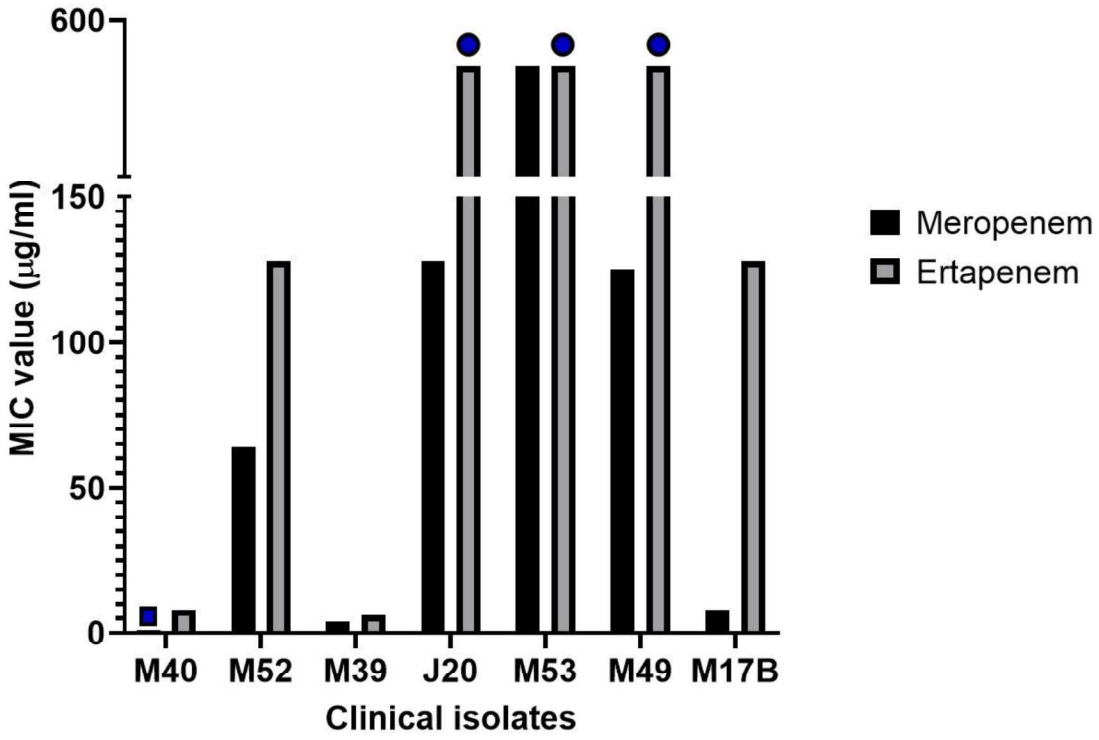

Figure 4.11 Minimum inhibitory Concentration of *K. pneumoniae* against carbapenem drugs. M40 (no carbapenemase gene), M52 (*bla*OXA-232), M39 (*bla*NDM-1), J20 (*bla*OXA-181), M53 (*bla*NDM-5), M49 *(bla*NDM-5 + *bla*OXA-181*)*, and M17B (*bla*NDM-1 + *bla*OXA-232). Square filled with blue colour indicates MIC value <1 µg/mL, Circle filled with blue indicates MIC value >512 µg/mL.

4.3.5.5 Molecular Docking of carbapenemase protein with carbapenem drugs

The protein structures of NDM-1, NDM-5, OXA-181, and OXA-232 were obtained and subjected to docking with carbapenem medicines, specifically meropenem and ertapenem. The docking analysis was conducted by considering the binding energy, hydrogen bonding, and RMSD value, as shown in **Table 4.3**.

Table 4.2 Docking results of meropenem and ertapenem with NDM-1, NDM-5, OXA-181, and OXA-232

No.	Compound	Protein	RMSD	Binding energy (kcal/mol)	No. of H bonds (Drug-Enzyme)	Amino acid involved in interaction
1.	Meropenem	NDM-1	0.000	-6.5	4	Val169, Pro171, Ala174, Pro175, Asn176, Phe177, Gly178, Leu180, Lys181
		NDM-5	0.000	-6.2	4	Trp93, His189, Cys208, Lys211, Asp212, Lys214, Ala215, Lys216, Ser217, Leu218, Gly219, His250, Ser251
		OXA-181	0.000	-6.9	3	Leu158, Ala69, Ser70, Ile102, Ala104, Trp105, Lys116, Tyr117, Ser118, Val120, Tyr211, Thr213, Arg214,
		OXA-232	0.000	-7.5	5	Ala69, Ser70, Lys116, Tyr117, Ser118, Val120, Leu158, Lys208, Thr209, Gly210, Tyr211, Leu247, Arg250
2.	Ertapenem	NDM-1	0.000	-7.5	4	Trp168, Val169, Pro171, Ala174, Pro175, Asn176, Phe177, Gly178, Leu180, Lys181, Val182, Asp199, Phe240
		NDM-5	0.000	-8.0	4	Trp168, Val169, Pro171, Lys181, Val182, Gly197, Ile198, Asp199, Thr201, Asp202, Ile203, Ala204, Ala239, Phe240, Pro241, Lys242, Ala243
		OXA-181	0.000	-7.6	3	Ser70, Ile102, Ala104, Trp105, Met115, Lys116, Tyr117, Ser118, Thr197, Ala207, Lys208, Thr209, Gly210, Tyr211, Trp222, Arg250, Gln251
		OXA-232	0.000	-9.1	8	Ala69, Ser70, Trp105, Lys116, Tyr117, Ser118, Val120, Leu158, Thr197, Ala207, Lys208, Thr209, Gly210, Tyr211, Trp222, Leu247, Arg250

4.3.5.5.1 Interaction of Meropenem with NDM-1, NDM-5, OXA-181, and OXA-232

Meropenem's docking score with NDM-1, NDM-5, OXA-181, and OXA-232 was -6.5, -6.2, -6.9, and -7.5 kcal/mol, in that order. As seen in **Figure 4.12**, hydrogen bonding, van der Waals interaction, and other interactions (Pi-Sigma and unfavorable acceptor-acceptor) were engaged and are what cause the binding. OXA-232's lower binding energy (-7.5) shows higher binding affinity than NDM-1's higher binding energy (-6.5), which denotes reduced binding affinity for meropenem medication.

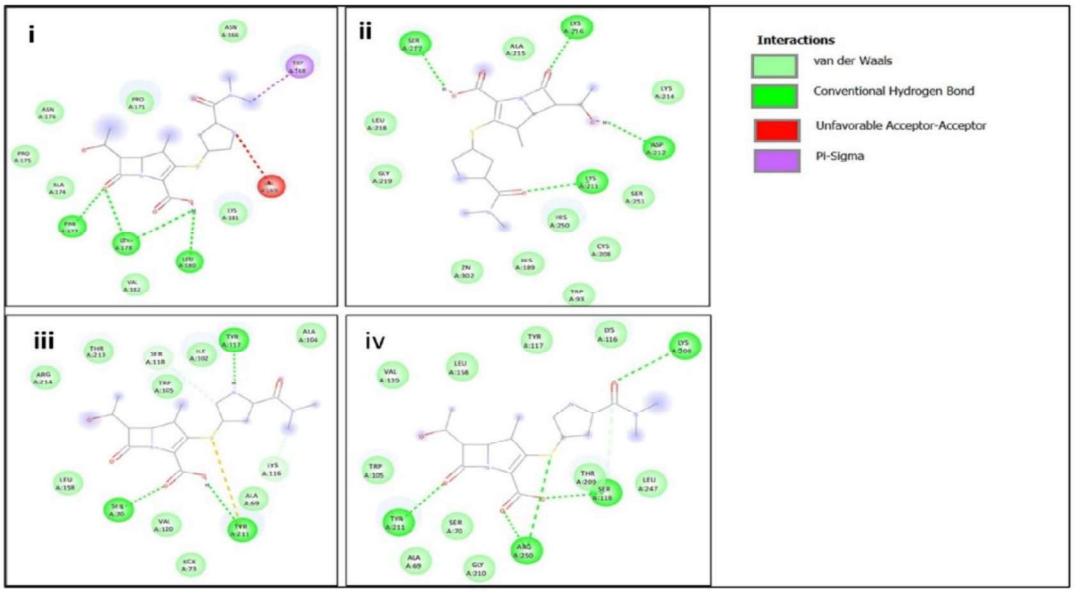

Figure 4.12 Two-dimensional figure showing the interaction of meropenem with carbapenem resistant proteins. It displays the low energy docking conformations of meropenem with four specific proteins: NDM-1, NDM-5, OXA-181, and OXA-232. The shown residues are engaged in hydrogen bonding (green) and van der Waals contact (light green). The green dashed line represents the phenomenon of hydrogen bonding.

4.3.5.5.2 Ertapenem's interactions with OXA-181, OXA-232, NDM-1, and NDM-5

The binding affinity, represented as the docking score, for ertapenem with NDM-1, NDM-5, OXA-181, and OXA-232 was -7.5, -8.0, -7.6, and -9.1 kcal/mol, respectively. Ertapenem had a lower affinity than meropenem for all four proteins, as shown by its lower binding energy. The results also imply that a larger number of amino acids were involved in the demonstrated interaction as shown in **Figure 4.13.**

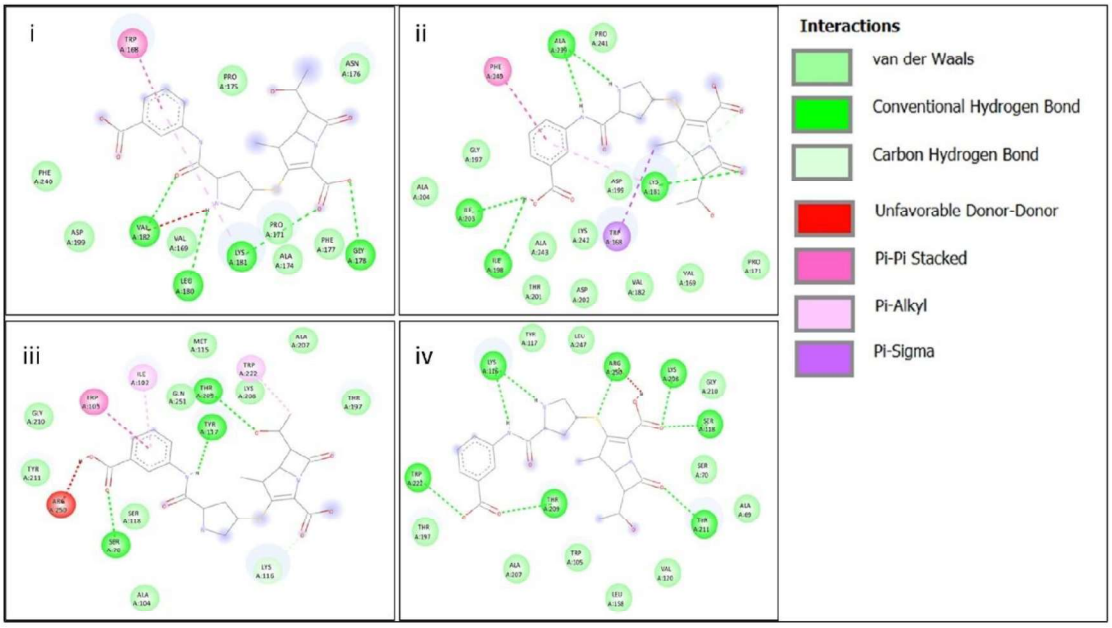

Figure 4.13 A 2D interaction diagram illustrates the docking of ertapenem with carbapenem resistant proteins. The figure shows the low energy docking conformations of ertapenem with NDM-1, NDM-5, OXA-181, and OXA-232. The displayed image shows the specific amino acid residues that participate in van der Waals interaction (light green) and hydrogen bonding (green). A green dashed line is used to symbolize hydrogen bonding.

4.3.6 Genomic study of the total resistance in lab isolates

The whole collection of AMR genes from all laboratory isolates was also examined and compared to their corresponding phenotypic patterns as shown in **Figure 4.14**. All the susceptible isolates had a resistance score of zero. None of these isolates possessed any genes associated with carbapenem and ESBL resistance, with the exception of isolate M25, which contained a single SHV-type gene from the ESBL class. Regardless of their drug resistance profile, all isolates had the *fosA* gene, which is responsible for fosfomycin resistance, and the *oqxA/B* genes, which are responsible for fluoroquinolone resistance. In the case of multidrug-resistant (MDR) isolates, the resistance score was either 1 or 0. Most of these isolates had genes *bla*OXA-1 and *bla*CTX-M-1-like, which are responsible for extended-spectrum beta-lactamase drug resistance. Surprisingly, one isolate, M39, from the MDR category carried the *bla*NDM gene, which is responsible for carbapenem resistance. In addition, they had *aac(3)*-types and *tet* genes that were accountable for aminoglycosides and tetracyclines. The *sul* and *dfrA* genes function as antagonists of the folate system and have also been identified in multidrug-resistant isolates.

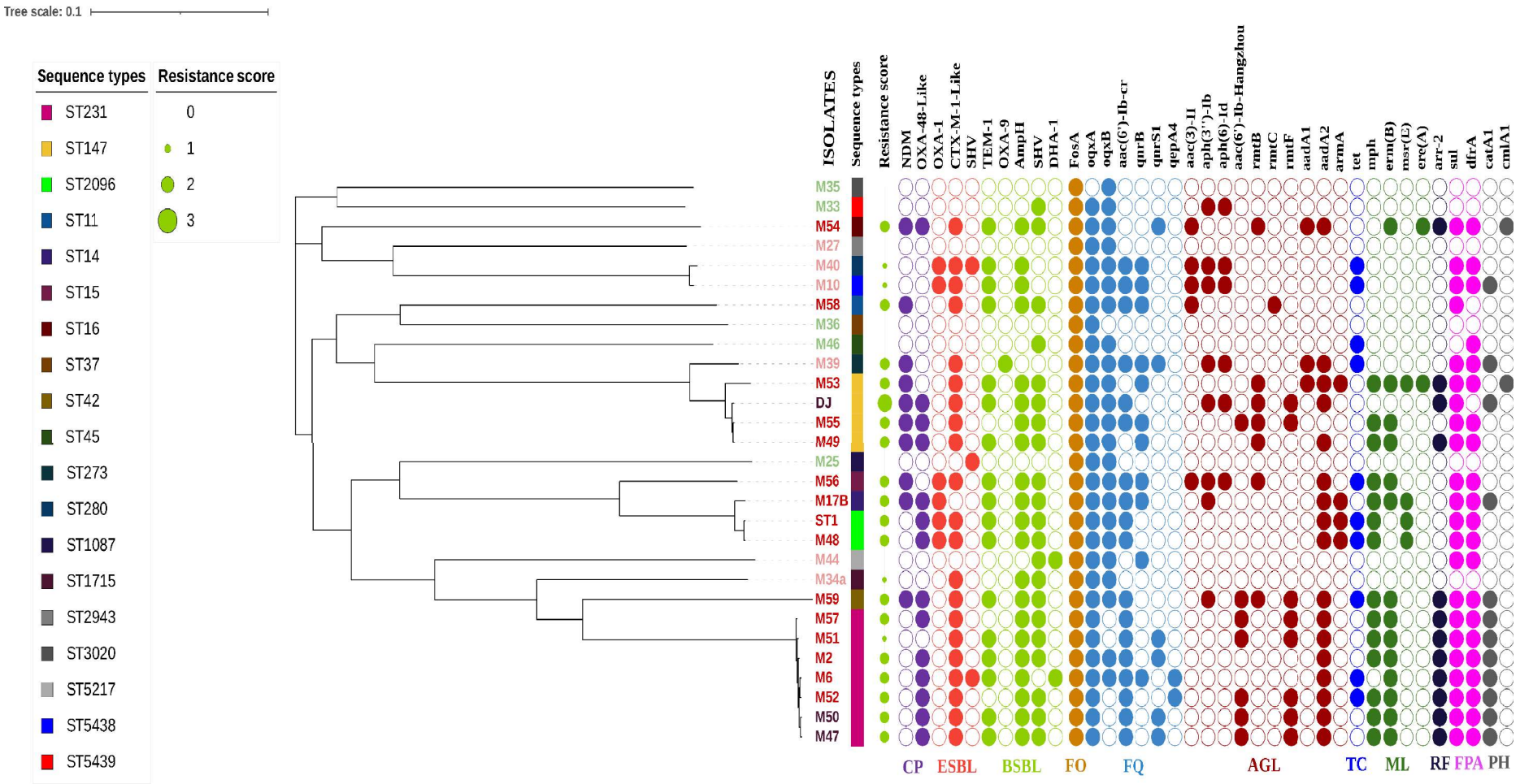

Figure 4.14 Total antibiotic resistance gene profile for different classes of antibiotics in lab isolates (*n* = 29). The isolates listed in various colors show their drug susceptibility profile: green for **susceptible**, light red for **MDR**, red for **XDR**, and dark red for **PDR.** In the resistance score, a bigger circle size signifies a higher resistance score, which in turn suggests a greater number of genes present in the genome. Circle filled with different colours indicates presence of that particular gene, while blank indicates absence of genes.

(Abbreviations: CP- carbapenems, **ESBL-** extended spectrum beta-lactams, **BSBL-** broad spectrum beta-lactams, **FO-** fosfomycin, **FQ-** fluoroquinolones, **AGL-** aminoglycosides, **TC-** tetracyclines, **ML-** macrolides, **RF-** rifampin, **FPA-** folate pathway antagonist, **PH-** phenicols).

All XDR isolates from our investigation had a resistance score of 2, with the exception of isolate M51. The XDR isolates exhibited the highest prevalence of carbapenemase genes (*bla*NDM and *bla*OXA-48-like), with the exception of M51. Apart from that, the majority of the isolates had at least one gene that could resist each class of antibiotics. It is unfortunate that only a few numbers of XDR isolates, namely M17B, M49, M54, M55, and M59, collected in 2020, with the exception of M17B, have dual carbapenemase genes. In the instance of PDR isolates, M47 and M50 have a resistant score of 2, whereas another PDR isolate DJ has a resistance value of 3. Furthermore, it is concerning that these isolates had several genes for broad-spectrum beta-lactam, fluoroquinolones, aminoglycosides, macrolides, and folate pathway antagonist drug classes. This genetic makeup has the potential to raise the minimum inhibitory concentration and exacerbate the severity of infections. To sum up the genetic and phenotypic links with sequence types, most of the XDR and PDR isolates belonged to ST231, ST147, and ST2096, which were the most common sequence types found in India.

We also investigated the genetics of colistin and tigecycline resistance in isolates that exhibited phenotypic resistance to colistin (M47, M48, M50, and DJ) and tigecycline (M47, M48, M49, M50, M51, M52, M53, M54, M55, M56, M57, M58, M59, and DJ). The known plasmid-mediated gene *mcr* was not discovered in any of the isolates. Disruption of the *mgrB* gene was detected in isolate DJ, which included a 1057bp insertion sequence (IS5), as previously indicated by the lab senior, whereas the *mgrB* gene was found to be intact in isolates M47, M48, and M50. Further, in the mutation study of two component systems, the amino acid sequences of PhoPQ and PmrAB were analyzed and found to be intact without any mutation except for PmrB. In isolates M47 and M50, a single common mutation (T246A) was observed when compared to a reference sequence of PmrB from the MGH 78578 strain of *K. pneumoniae*, where threonine was substituted by alanine at position 246 as shown in **Figure 4.15**. However, even after analyzing the major genes responsible for colistin resistance, the reason for resistance in isolate M48 was unknown. This suggests that there could be other possible molecular mechanisms, or overexpression of efflux pumps, that lead to the colistin resistance in isolate M48.

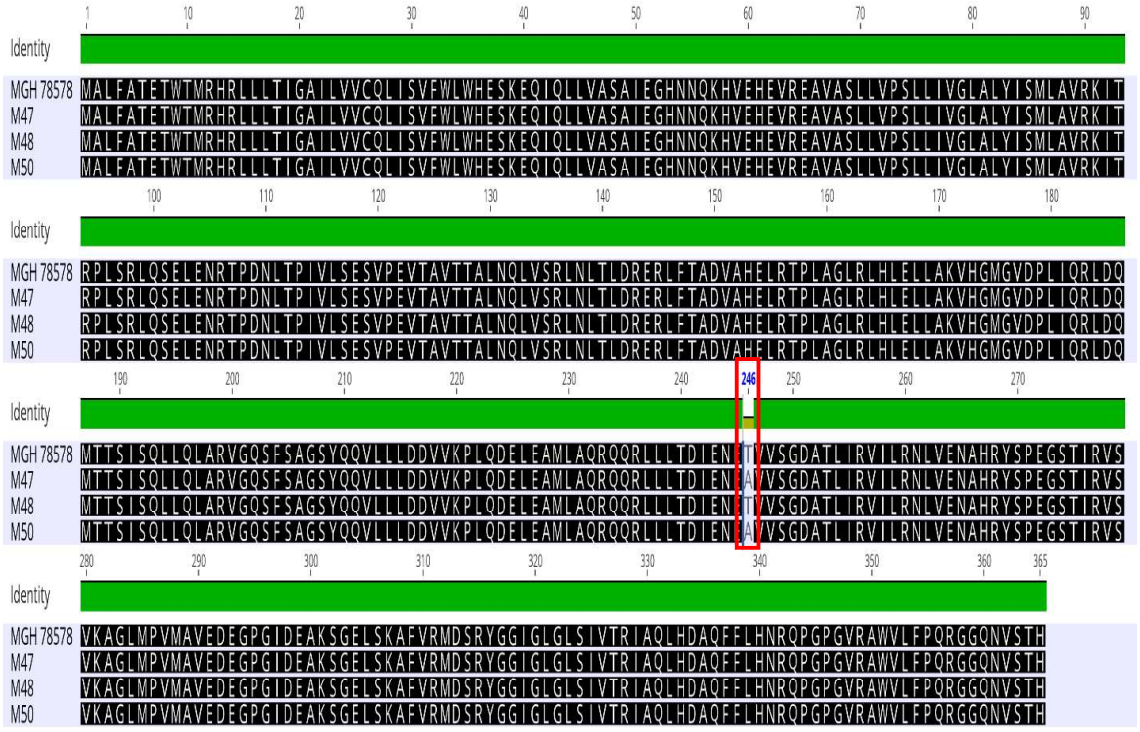

Figure 4.15 Alignment of amino acid sequence of PmrB protein. Isolate M47, M48, and M50 was aligned against reference strain MGH 78578; all sequences were perfectly matched except mutation (T→A) at position 246 in M47 and M50. A thick green line indicates the consensus sequences; a black color indicates a perfectly aligned sequence; and while indicates a mutation or mismatch.

A mutation in the protein sequence of the *ramR* gene was examined in order to comprehend the molecular mechanism of tigecycline resistance. All isolates resistant to tigecycline, with the exception of M49, were determined to have at least one single mutation in their amino acid sequence. On the other hand, M49 demonstrated gene disruption inactivation, wherein the *ramR* gene was disrupted into two segments and identified in distinct contexts as depicted in **Figure 4.16**.

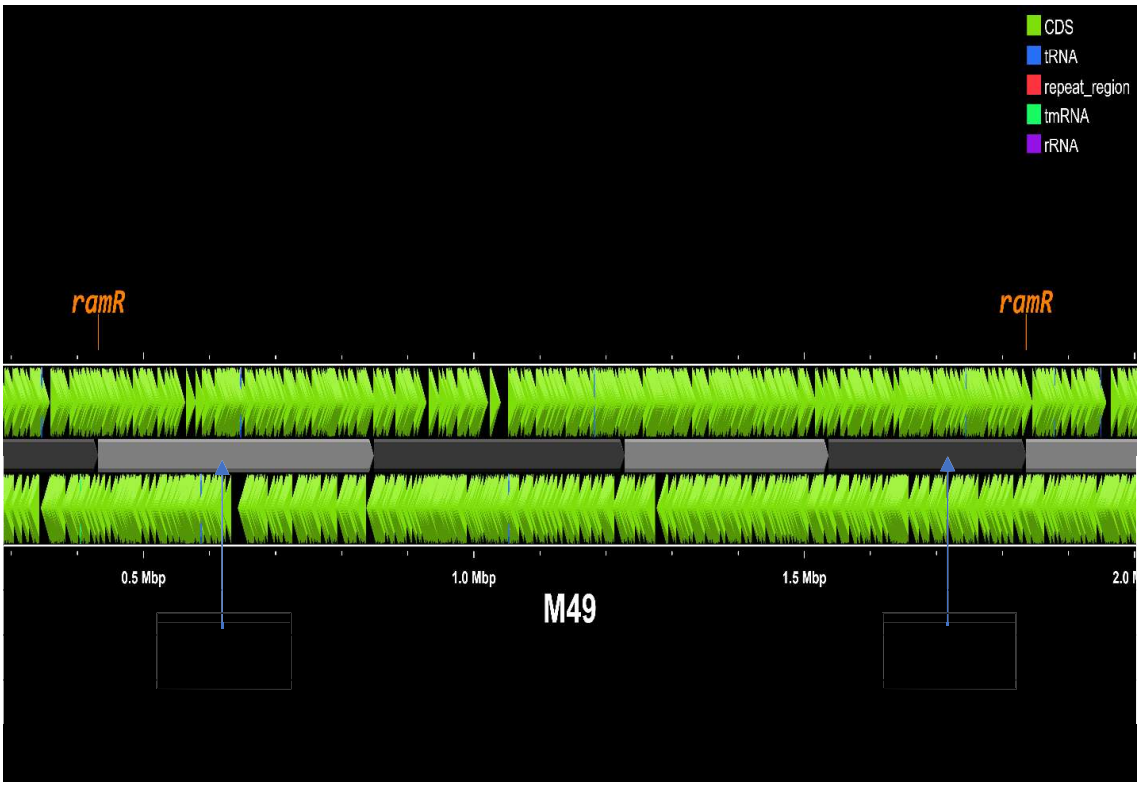

Figure 4.16 Disruption of *the rmrR* gene in isolate M49. The *ramR* gene was detected in two fragments, one at contig 2 and another at contig 5. The green triangle arrow indicates the coding sequences; Black and Grey segments indicate contigs.

As depicted in **Figure 4.17,** the mutation M184V was the most common and detected in 5/14 tigecycline-resistant isolates. Isolates M47, M50, M51, M52, and M57 had the M184V mutation, where methionine was substituted by valine in the 184th position. Followed by R3S (Arginine substituted by Serine) and A173V (Alanine substituted by Valine) mutations detected in M55, DJ, and M47, M50, respectively. Dual mutation was also observed in M47 (A173V, M184V), M50 (A173V, M184V), M56 (A19V- Alanine substituted by Valine, G25S- Glycine substituted by Serine), and M59 (R35C- Arginine substituted by Cystine, A105S- Alanine substituted by Serine). Whereas other single mutations, K9I (lysine substituted by isoleucine), were detected in M48, A72P (alanine substituted by proline) in M53, I141T (isoleucine substituted by threonine) in M54, and A153T (alanine substituted by threonine) in M58.

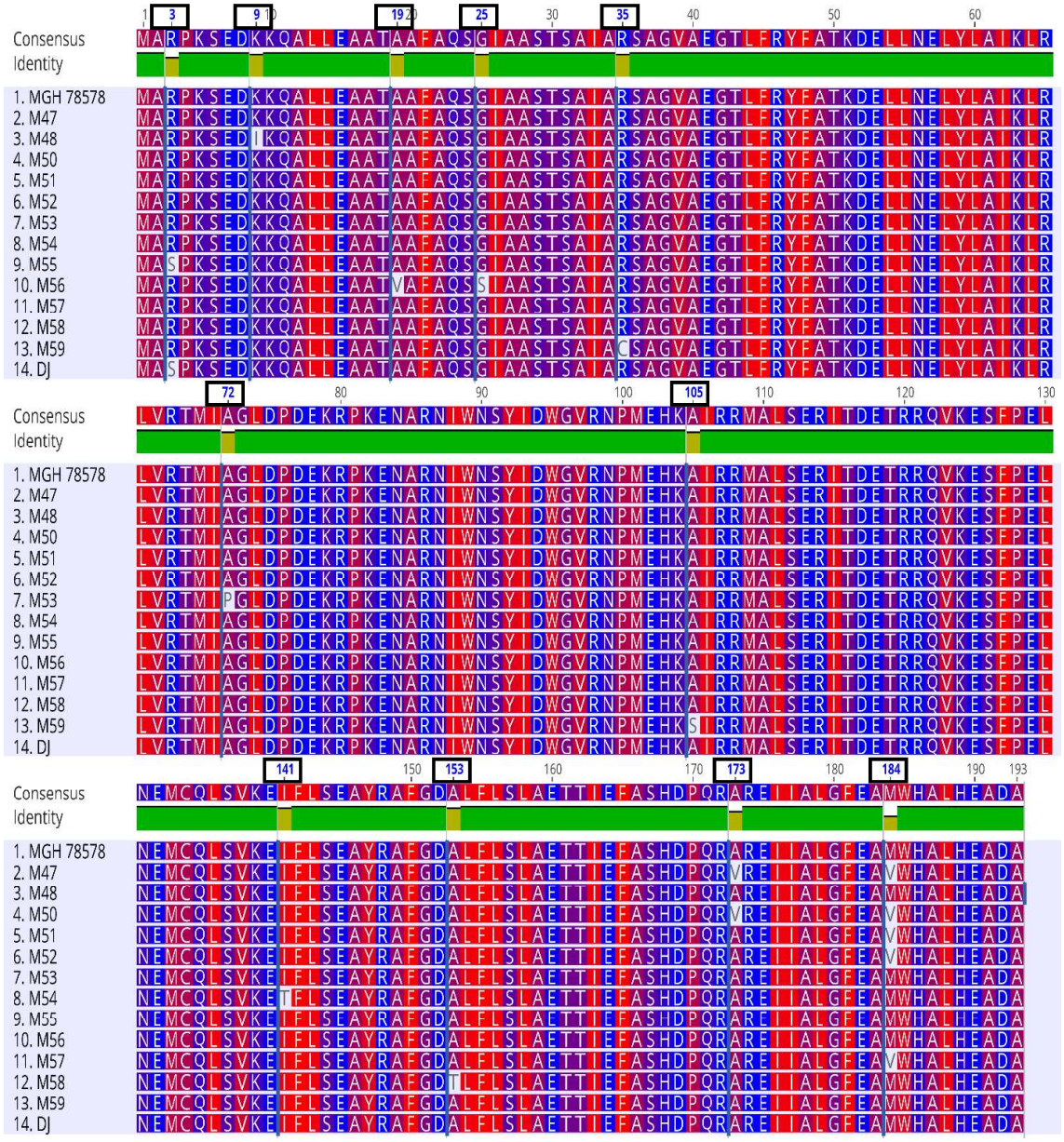

Figure 4.17 Study of mutation in sequence of ramR protein. The amino acid sequence of ramR from all tigecycline-resistant isolates was alligened against reference strain MGH 78578. All isolates consisted of at least one mutation and were highlighted in white. All mutated regions were indicated in number with blue font and black square.

4.3.7 Investigating the dynamics of prophages and their impact on the formation of biofilms in *Klebsiella pneumoniae*.

4.3.7.1 Detection of prophages in K. pneumoniae genomes (Lab isolates)

The PHASTER tool was utilized to detect and categorize the prophage in all the genomes. **Figure 4.18** displays a circular genome of M53 as an example. **Figure 4.18(B), (C),** and **(D)** demonstrate the three categories of prophages: incomplete, intact, and questionable, respectively. A variance in the total number of prophages was observed among the isolates, with a range of 2 to 11. As shown in **Figure 4.19,** apart from M36 and M39, all isolates possessed intact prophages inside their genome. The range of intact prophages observed ranged from 1 to 6. Interestingly, various types of prophages have been discovered in the genomes of *K. pneumoniae*. These prophages are categorized as '*Klebsiella*' prophages and are referred to as "Klebsi". Additional prophages that were identified did not belong to the *Klebsiella* genus. These prophages are referred to as 'other than *Klebsiella* (OTK)' prophages and include "Salmon", "Escher", "Entero", "Cronob", "Erwini", "Phage," "Pectob", and others. Eight unique "Klebsi" phages were detected, namely PHAGE_Klebsi_phiKO2_NC_005857 and PHAGE_Klebsi_ST147_VIM1phi7.1_NC_049451, which were the most prevalent. These phages were present in eight genomes of *K. pneumoniae*.

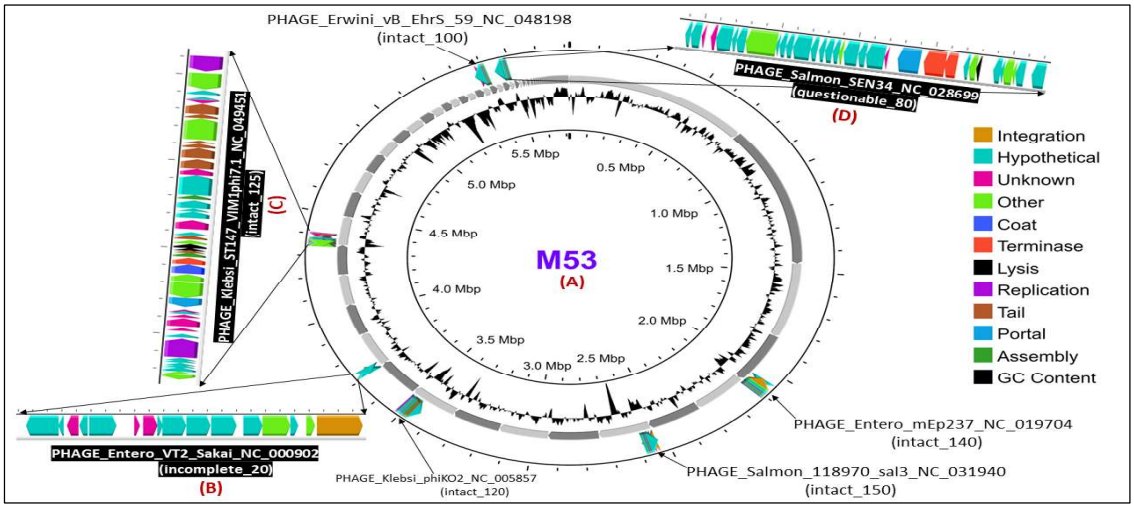

Figure 4.18 Circular genome of a representative strain (M53) with the prophages. (B) denotes incomplete prophages with a score of 20, (C) denotes entire prophages with a score of 125, and the (D) denotes questionable prophage with a score of 80 detected in genome of M53 isolate.

A total of 53 distinct varieties of OTK phages were identified. The frequently appearing phage was PHAGE_Salmon_118970_sal3_NC_031940, with a count of 16. This was followed by PHAGE_Escher_500465_1_NC_049342 and PHAGE_Escher_RCS47_NC_042128, all with a count of 14. PHAGE_Entero_c_1_NC_019706 had a count of 11, while PHAGE_Entero_mEp237_NC_019704 had a count of 10. (Adriaenssens & Brister, 2017) propose a nomenclature for prophages that includes the complete name of the host genus, followed by the term "phage," and a distinctive identifier, such as PHAGE_Klebsi_ST15_OXA48phi14.1_NC_049454. The prophages identified in the genomes of *K. pneumoniae* are presented in **Table 8.1 (See Appendices)**.

There was n = 25 "Klebsi" phages identified in the study. Out of them, 20 (80%) were intact phages and were discovered in the second most prevalent sequence type, ST147, as well as in many other less frequent sequence types: ST5438, ST5217, ST2096, ST1715, ST1087, ST280, ST42, ST16, ST15, and ST11. It is noteworthy that the ST231 strain, which is the most common ST type, does not possess any "Klebsi" phages in its genetic makeup. The genetic composition of all four strains of ST147, together with additional strains of ST42 and ST16, consisted of two fully functional phages. All "Klebsi" prophages discovered in the genomes of *K. pneumoniae* were situated on the chromosome, except for a PHAGE_Klebsi_phiKO2_NC_005857 prophage that was detected on plasmids in ST147 and ST42.

Regarding prophages other than *Klebsiella* (OTK), n = 169 prophages were identified across genomes. Out of the total, 56 (33.13%) were intact, 27 (15.97%) were questionable, and 87 (51.47%) were incomplete. The predominant intact phage found in OTK samples was PHAGE_Entero_c_1_NC_019706. We found all occurrences of this phage on chromosomes, and interestingly, except for one, we detected it in either ST231 or ST147. The phage PHAGE_Salmon_118970_sal3_NC_031940 was the second most frequently detected, occurring in 7 genomes. Afterwards, six distinct genomes detected PHAGE_Entero_mEp237_NC_019704 and PHAGE_Erwini_vB_EhrS_59_NC_048198. All of them were located on the chromosomes. Furthermore, we primarily found them in ST231 and ST147, with a few other infrequent STs present. We discovered all phages integrated into a chromosome, except for the three PHAGE_Salmon_SSU5_NC_018843 and one PHAGE_Entero_I2_2_NC_001332. All four intact phages found on plasmids belonged to ST231 and ST147. Out of the questionable phages, PHAGE_Escher_500465_1_NC_049342 was the most prevalent. These phages were all located on the chromosome and randomly distributed among the STs. The predominant incomplete phage,

PHAGE_Escher_RCS47_NC_042128, was found in 13 genomes exclusively on plasmids and dispersed randomly across various sequence types. The chromosome revealed the second most prevalent phage, PHAGE_Salmon_118970_sal3_NC_031940, while the plasmid revealed PHAGE_Salmon_SJ46_NC_031129. Interestingly, most of the OTK phages discovered on plasmids were of the incomplete type.

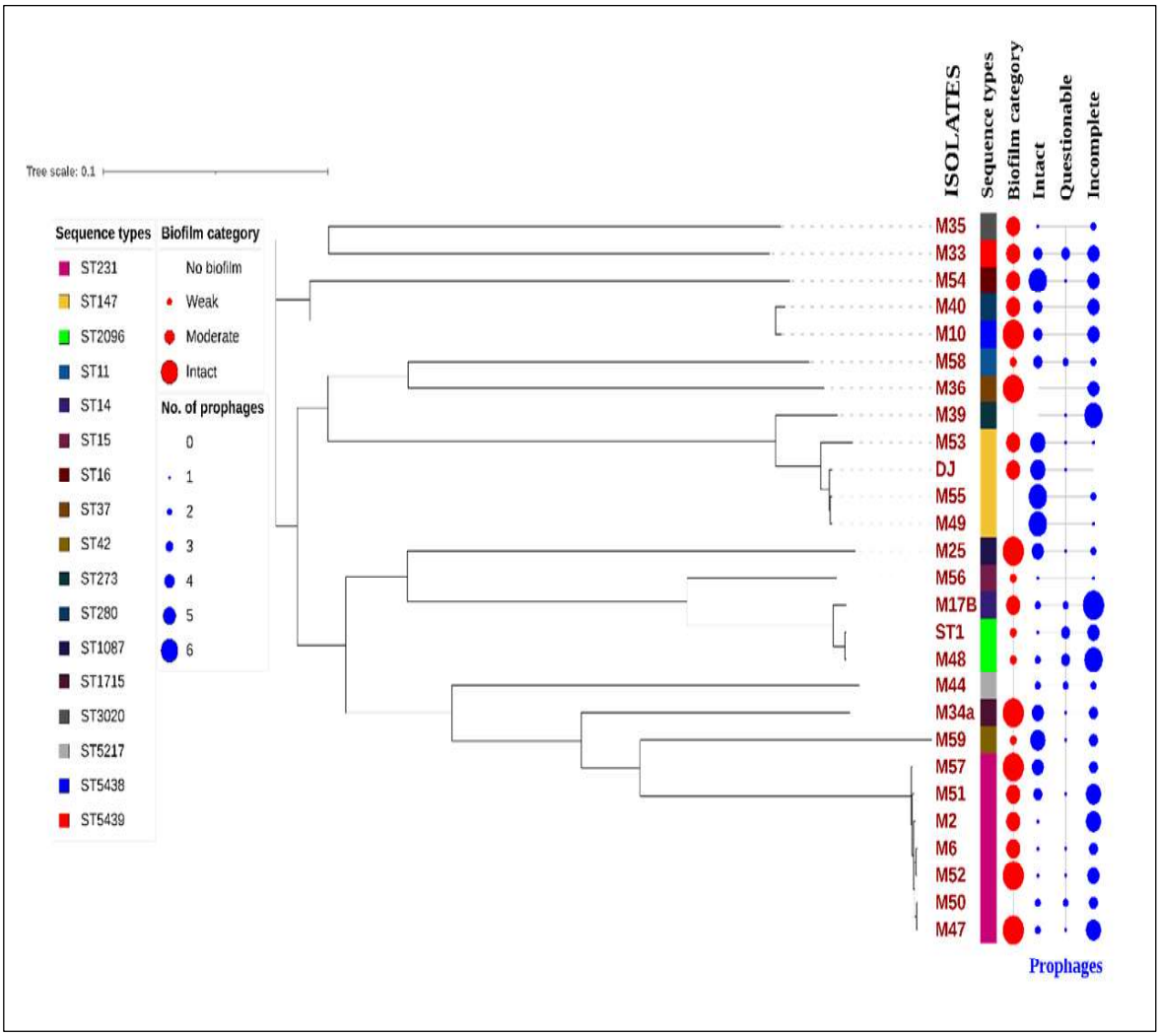

Figure 4.19 Biofilm category of laboratory isolates and the presence of prophage elements in the genomes of clinical isolates of *K. pneumoniae* from the laboratory (*n* = 27). The red color and round shape represent the biofilm category, with bigger sizes indicating stronger biofilm categories. The blue color and round shape represent the number of prophages found across *Klebsiella* genomes, with larger sizes indicating a higher number and smaller sizes indicating a lower number. However, the blank signifies the isolates that do not form biofilms, and no genomes of prophages were found.

4.3.7.2 Biofilm assay for categorization of isolates

The biofilm was categorized using the crystal violet assay. Biofilms were divided into four groups: non-biofilm-forming, weak, moderate, and strong. Five weak (M48, M56, M58, M59, and ST1) ten moderates (M2, M6, M17B, M33, M35, M40, M51, M53, M54, and DJ) seven strong (M10, M25, M34a, M36, M47, M52, and M57) and five non-biofilm (M39, M44, M49, M50, and M55) forming isolates were discovered as shown in **Figure 4.19 and Figure 4.20.**

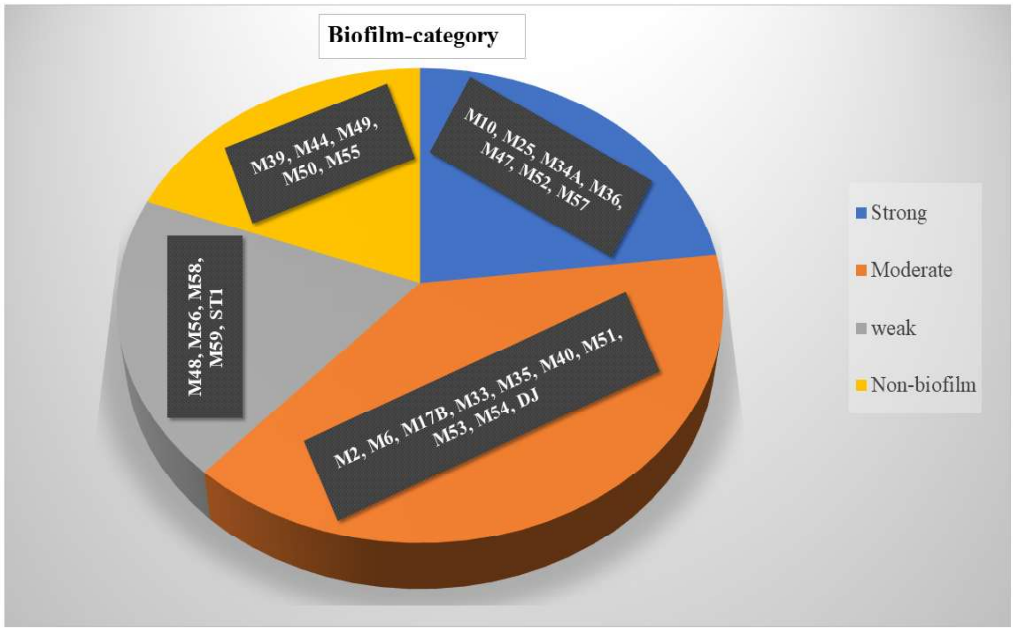

Figure 4.20 Classification of isolates according to their biofilm formation capability. There were Five isolates each were categorized as non-biofilm forming and weak, n = 10 isolates were moderate biofilm forming, while n = 7 isolates were strong biofilm forming.

4.3.7.3 Growth Curve for optimization of concentration of MMC of selected isolates

We have optimized the concentration of MMC in order to assess the viability of the isolates (M6, M10, M36, DJ, M52, M53, M55, and M57). These adjusted MMC concentrations may then be used for the prophage induction experiment. In the growth curve experiment, the optical density (O.D.) of all the chosen isolates was nearly like the control when exposed to 1µg/ml and 3µg/ml. However, significant cell mortality was seen in all isolates, except for M10, when treated with 5µg/ml of MMC **(Figure 4.21)**. Therefore, the concentrations of 1ug/ml and 3ug/ml of MMC were chosen for prophage induction.

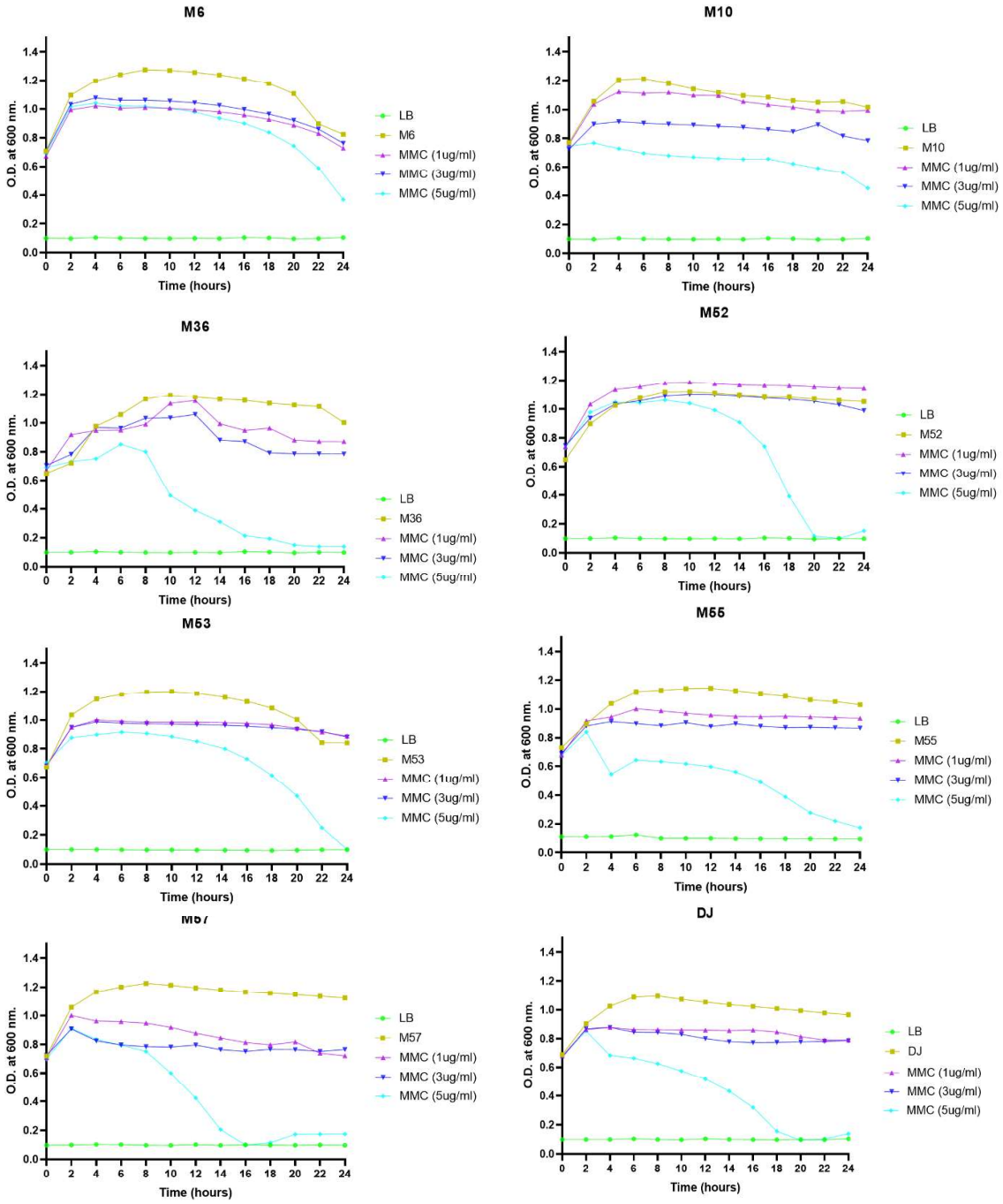

Figure 4.21 Growth curve of representative isolates in presence of mitomycin C. Isolate's M6, M10, M36, M52, M53, M55, M57, and DJ growth pattern in response to various concentrations of MMC (1 ug/ml, 3 ug/ml, 5 ug/ml) were shown, and all isolates were growing well nearly equivalent to control in presence of MMC with the concentrations of 1 ug/ml and 3 ug/ml, whereas cell death can be observed at concentrations of 5 ug/ml in isolates.

4.3.7.4 Prophage induction and biofilm assay

Further, Prophage induction was done at 0 µg/ml, 1 µg/ml, and 3 µg/ml for eight isolates M6, M10, M36, M52, M53, M55, M57, and DJ. However, the best plaque was seen at 3 µg/ml MMC in all isolates except M36 (had no intact or questionable phages) as shown in **Figure 4.22 (A) and (B)**.

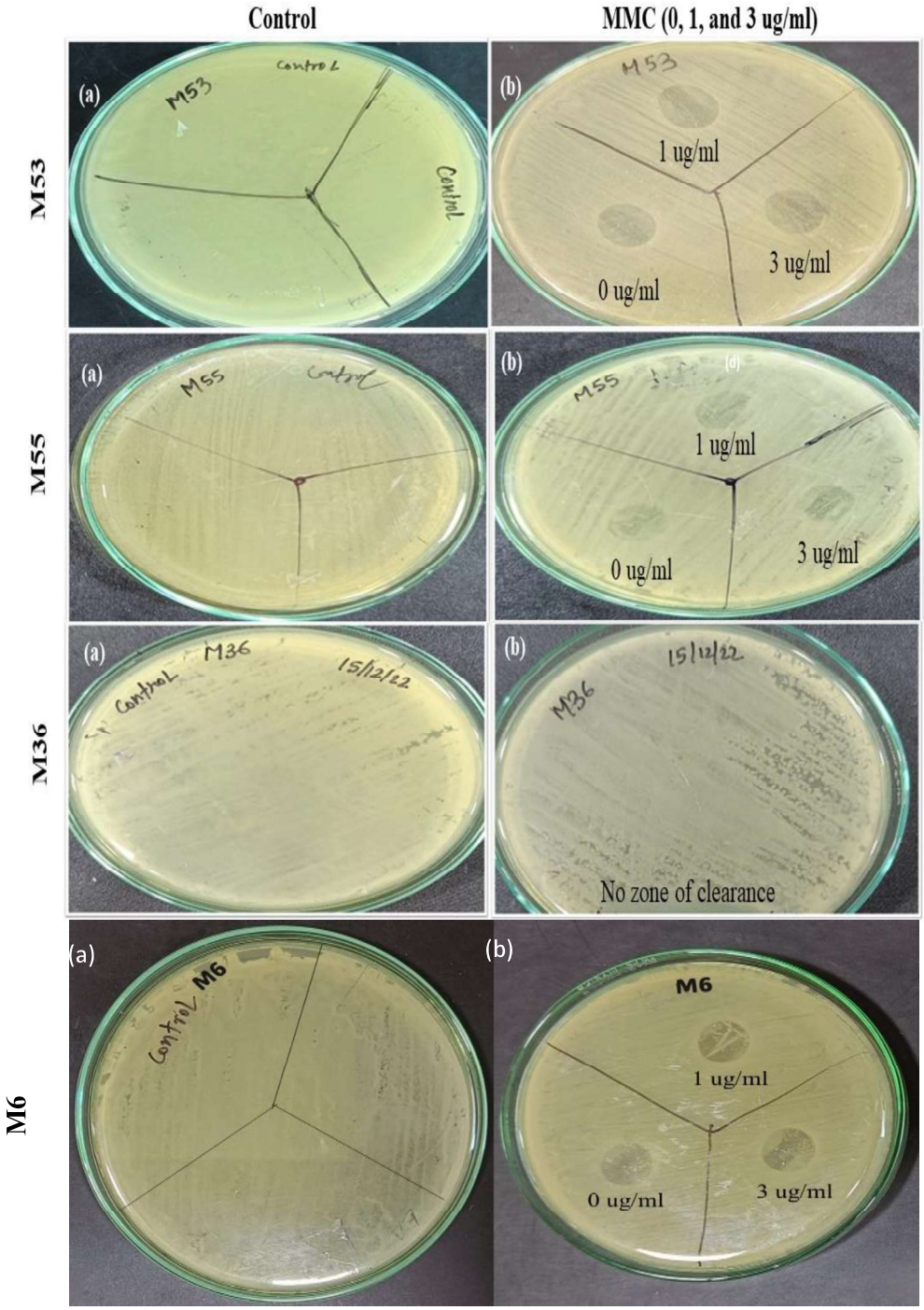

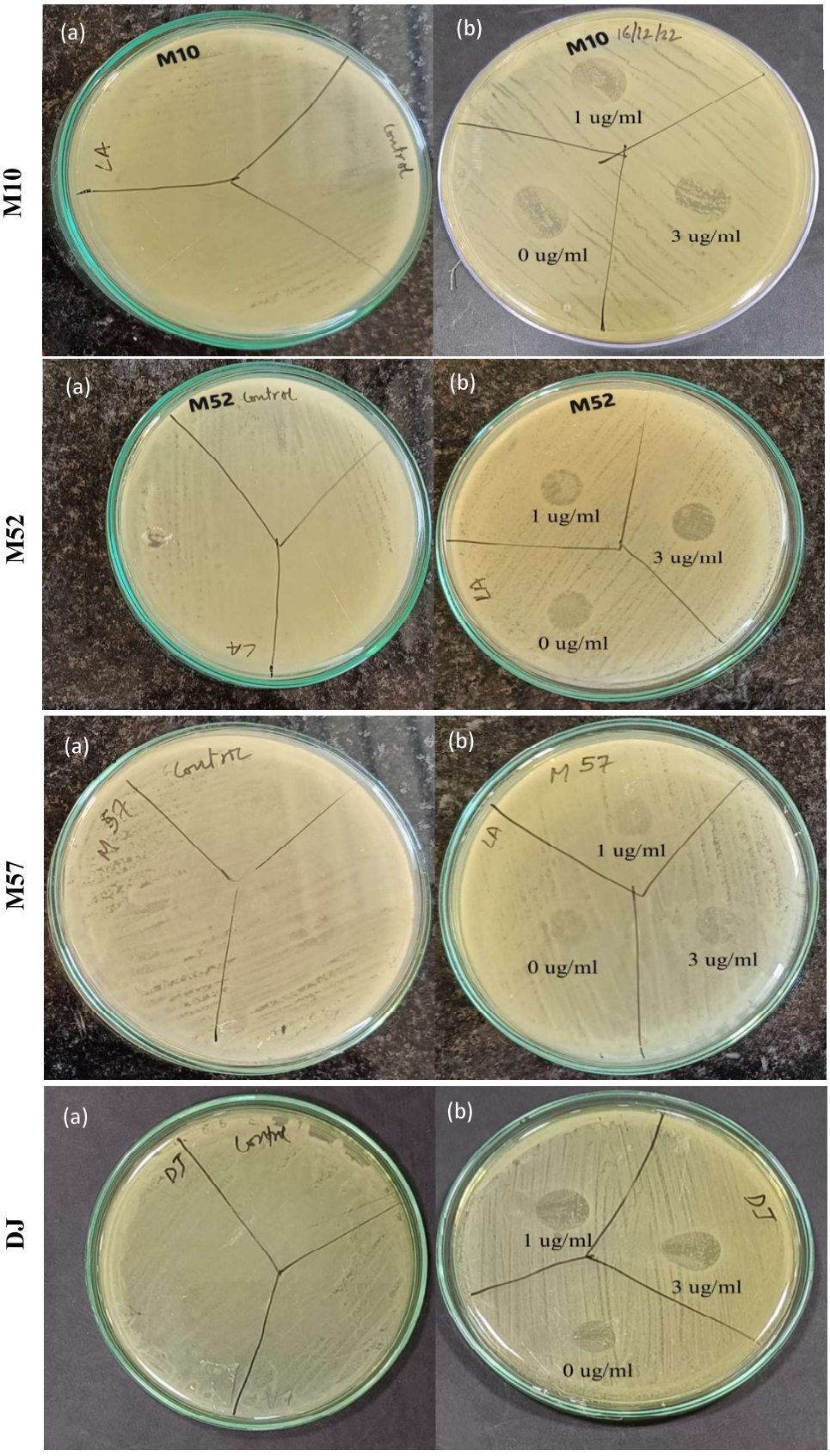
M10
M52
M57
DJ
(a)
(b)
M10
M10 16/12/22
1 ug/ml
3 ug/ml
0 ug/ml
LA
Control
M52
M52 Control
M 57
DJ

(A)

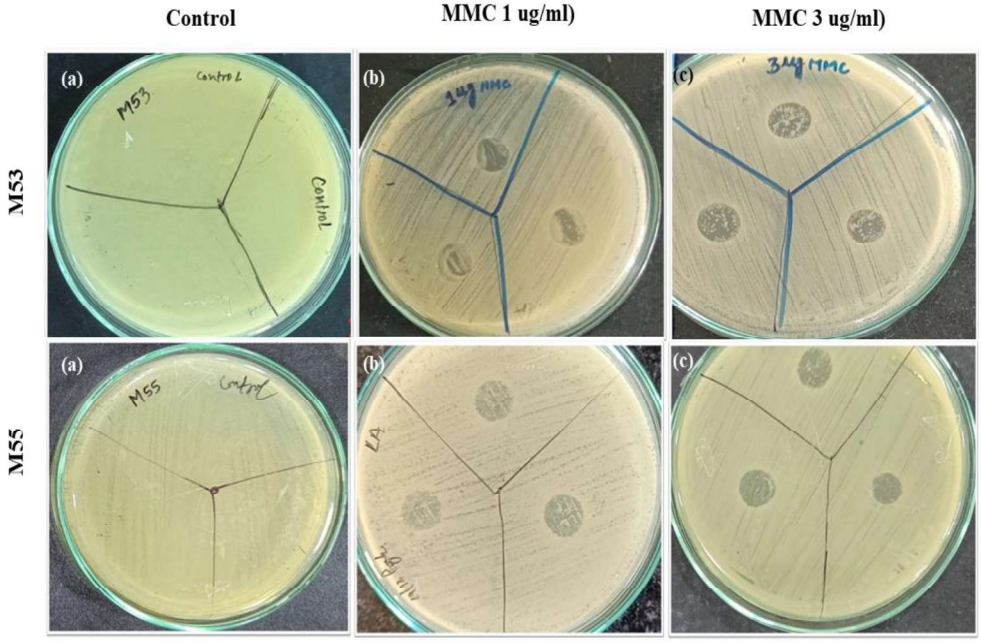

(B)

Figure 4.22 Image of isolates M53, M55, M36, M6, M10, M52, M57, and DJ tested for prophage induction. (A) depicts the isolates that were grown without any treatment (a), (b) shows the isolates that were grown and treated with 0, 1, and 3 ug/ml MMC. As the amount of MMC rose, the severity of the Zone of Clearance in Isolates M53, M55, M6, M10, M52, M57, and DJ also increased. However, at any given concentration, the isolate M36 did not exhibit a clear zone. (B) shows the results in triplicates, with (b) displaying the isolates that received treatment with 1 ug/ml MMC and (c) displaying the isolates that received treatment with 3 ug/ml MMC. The isolates M53 and M55 demonstrated superior clearance efficacy at a concentration of 3 ug/ml compared to 1 ug/ml.

A biofilm assay was conducted to investigate the impact of prophage induction on the production of biofilms. A correlation between prophage inductions and a decrease in biofilm formation was seen, except for strains M55 and M10. The graph illustrates a decrease in the optical density (O.D.) value at concentrations of 1µg/ml and 3µg/ml, except for M55 and M10, as indicated in **Figure 4.23.** The significant decrement of O.D. at 3 ug/ml was observed in isolates M52, M6, M53, DJ and M36, However the significant reduction was seen at 1 ug/ml concentration in M52, M53, DJ and M36. Whereas the reduction of O.D. at both the

concentrations in isolate M57 was non-significant. Surprisingly the isolate M10 and M55 showed the significant increase of O.D. at both the concentrations 1 ug/ml and 3 ug/ml of MMC.

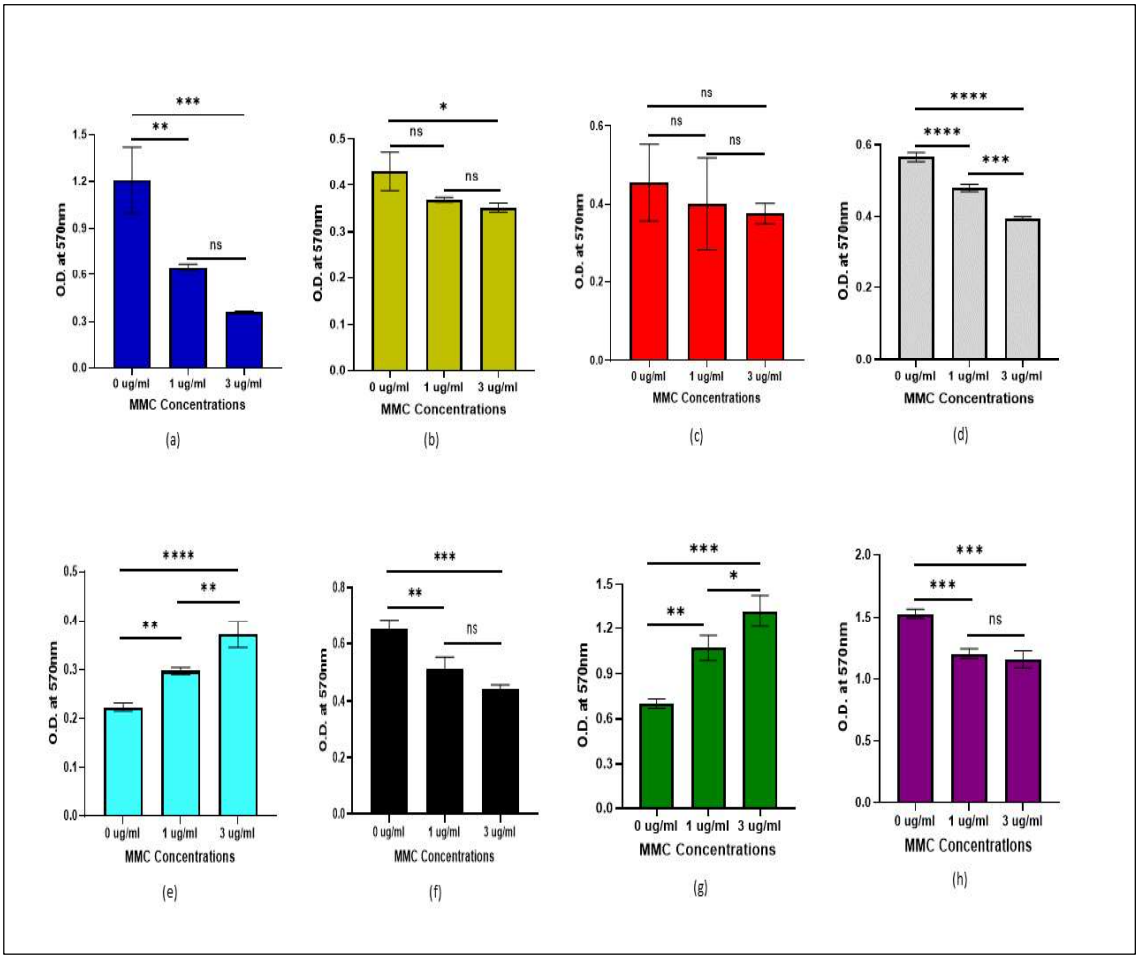

Figure 4.23 Impact of prophage induction on biofilm. A biofilm assay was conducted to investigate using (a) M52, (b) M6, (c) 57, (d) M53, (e) M55, (f) DJ, (g) M10, (h) M36, isolates to check the impact of prophage induction on the production of biofilms. There seems to be a correlation between prophage inductions and a decrease in biofilm formation, except for strain (e) M55 and (g) M10. A notable decrease in optical density (O.D.) was observed (a) M52, (d) M53, (f) DJ, and (h) M36, while a considerable increase was observed in (e) M10 and (f) M55. Statistical analysis was conducted using a one-way ANOVA with GraphPrism 8.4.2. *p<0.05; **p<0.01; ***p<0.001; ****p<0.0001; no significance p>0.05.

4.4. Discussion

β-lactams are often recommended antibiotics for the treatment of *Klebsiella* infections, whereas carbapenems are a class of medications that are used as a last option to treat strains of the bacteria that are extremely resistant to other antibiotics. The emergence of carbapenem-resistant *K. pneumoniae* poses an imminent danger to public health. WGS is being used in research and public health laboratories to efficiently and cost-effectively monitor infections and resistance. The current investigation found that 72.24% (n = 151) of isolates included at least one carbapenemase gene (either *bla*OXA or *bla*NDM), whereas 19.20% (n = 29) of isolates had both carbapenemase genes present in their genome.

The study identified two primary categories of carbapenemase genes, particularly *bla*OXA-48-like and *bla*NDM-1/5. These genes were mostly linked to ST231 and ST147, respectively. As of 10 July 2024, a total of 60 different variants of *bla*OXA-48-like and 65 different variants of *bla*NDM have been documented. This information is available at https://www.ncbi.nlm.nih.gov/pathogens/refgene. However, it is fortunate that only four variations of *bla*NDM and three variations of *bla*OXA-48-like were found in the genomes of Kp bacteria that are now spreading in India.

India's recent genetic surveillance research mostly focused on South India (Shankar et al., 2019, 2022a; Sundaresan et al., 2022). Based on our current understanding and analysis of the genome databases, this work marks the inaugural inclusion of *Klebsiella* genomes from Western India in a surveillance investigation. The results of our research align with previous studies, as we also identified ST231 and ST147 as the most prevalent sequence types. However, we saw a discrepancy in the third most frequent ST, which we determined to be ST2096, while past studies reported ST14 as the third most common. Subsequently, we identified *bla*OXA-232 as the predominant carbapenemase, with a strong correlation to ST231. Comparable findings have been documented in both South and North India (Shankar et al., 2019; Naha et al., 2021). The fast spread of *bla*OXA-232 in ST231 may be linked to the wide range of mobile genetic elements located near *bla*OXA-232/181. These elements consist of several insertion sequences and transposons from the Tn3 family (Shankar et al., 2022a).

The *bla*OXA-232 gene was first detected in *K. pneumoniae* and *Escherichia coli* obtained from three individuals who relocated from India to France in 2011 (Potron et al., 2013). Subsequently, there have been global reports of *bla*OXA-232 Kp outbreaks, with many sequence types (STs) discovered. These include ST231 and ST2096 in France (Emeraud et al., 2022), ST16 in Thailand (Abe et al., 2022), ST147 in Germany (Xanthopoulou et al., 2020), ST14 and ST15 in China (Jia et al., 2021), ST307 and ST101 in The Netherlands (Hendrickx

et al., 2021), and ST437 and ST395 in India. We identified 24 genomes with *bla*OXA-181 and 2 ST101 genomes with *bla*OXA-48, both of which belong to the *bla*OXA-48-like group. Also, researchers identified *bla*OXA-48-producing *K. pneumoniae* strains from Europe and Africa as belonging to sequence type 395 (ST395) (Potron et al., 2013).

Currently, *bla*OXA-181 is regarded as the second most prevalent *bla*OXA-48-like variant worldwide, behind *bla*OXA-48 (W. Wu et al., 2019a). Prior to 2007, *bla*OXA-181 was prevalent in India and was identified as the predominant *bla*OXA-48-like carbapenemase. However, there is a possibility that the reporting of *bla*OXA-181 was inaccurate due to a limited and selective collection of samples from a small number of sites that had molecular diagnostic capabilities. Based on the current situation, it is clear that *K. pneumoniae* carrying *bla*OXA-232 and *bla*OXA-181 are widespread in India, with a larger occurrence of *bla*OXA-232, as found in the research. The *bla*OXA-48 enzyme is now the most prevalent *bla*OXA-48-like enzyme worldwide, with *bla*OXA-181 being the second most frequent (W. Wu et al., 2019a).

It is noteworthy that although *bla*OXA-181 was first discovered in India, its current incidence is lower in comparison to *bla*OXA-232. *bla*OXA-232 differs from *bla*OXA-181 due to a single amino acid substitution. Initially, the genetic surroundings of *bla*OXA-232 closely resembled those of *bla*OXA-181 (Pitout et al., 2019). It was possible for *bla*OXA-232 to have evolved from *bla*OXA-181 via a shared origin and transposition, as shown by the similarities between the genes, transposons, and plasmids of the two organisms. However, the MGEs linked to *bla*OXA-232 indicate that, over the last ten years, the genetic environment of the gene (particularly from India) has become very diverse (Shankar et al., 2022a). To provide a comprehensive understanding of the interactions that led to the effective distribution of *bla*OXA-232 (especially in ST231) and not *bla*OXA-181/48 in India, further long-read sequencing studies including a larger number of isolates from that country are necessary.

An additional significant finding in the current analysis was the presence of 29 isolates that simultaneously carried the genes *bla*OXA-48-like and *bla*NDM-1/5. The occurrence of the *bla*NDM-5 + *bla*OXA-232 combination was the most frequent, with a total of 11 instances, out of the 29 dual-producers. Only two genomes, namely B35725 and SBS12, of ST147 were identified to possess the combination of *bla*OXA-181 and *bla*NDM-5 carbapenemase genes on their chromosomes. The other dual producers had both genes on plasmids. The ST16 genomes in this investigation were found to coexist with *bla*NDM-5 and *bla*OXA-181. Additionally, reports of dual carbapenemase production have come from Algeria, Saudi Arabia, Iran,

Algeria, Italy, South Korea, and Saudi Arabia (Shibl et al., 2013; Cho et al., 2015; Avolio et al., 2017; Solgi et al., 2020; Chaalal et al., 2021).

The *bla*NDM-5 gene was predominantly present in genomes of the ST147 strain, which were associated with bloodstream infections in Tamil Nadu. On the other hand, genomes of the same ST147 strain were discovered to possess the *bla*KPC-2 gene, which was associated with respiratory tract infections in West Bengal. Interestingly, only the ST147 isolates that produced *bla*KPC-2 had the plasmid replicon IncFIB(K)(pCAV1099-114). The percentage of *bla*NDM-5 that coexisted with *bla*OXA-48-like was 65.78% (n = 25/38). It was reported that patients with *bla*OXA-48-like and *bla*NDM-5 had visited India or the Indian subcontinent from South Korea, the United States, and Nepal (Cho et al., 2015; Rojas et al., 2017; Sherchan et al., 2020).

The existence of carbapenemase duplexes (*bla*OXA-48-like and *bla*NDM-1/5) within the genomes may result in the emergence of pan-carbapenem-resistant isolates. Therefore, it is necessary to investigate the factors contributing to the formation of these duplexes to effectively address and combat them. A multinational group assessed the global prevalence and genetic diversity of human clinical samples of *bla*NDM-producing *K. pneumoniae* and discovered that *bla*NDM was detected in all five continents and was distributed across many sequence types (Safavi et al., 2020).

Previously, the absence of any prevailing lineages indicates that there are no *bla*NDM-positive *K. pneumoniae* clones of any significance clearly of significant concern. Recently, there has been a common occurrence of *bla*NDM-positive *K. pneumoniae* strains being described in association with ST14 (Giske et al., 2012; Yoon et al., 2018; Pitout et al., 2019). ST11 is a commonly observed sequence type in several examinations (Giske et al., 2012; Pitout et al., 2019). It is important to mention that ST11, which is the predominant sequence type of carbapenem-resistant *K. pneumoniae* in China, mostly harbors the *bla*KPC-2 gene rather than the *bla*NDM gene. While there is no data to definitively establish that ST11, ST14, ST15, and ST147 are epidemic clones responsible for the worldwide dissemination of *bla*NDM, their widespread occurrence in several countries necessitates further investigation (Qi et al., 2011). While *bla*NDM has been detected on bacterial chromosomes (Baraniak et al., 2016; Rodrigues et al., 2022) it is mostly carried on plasmids, which are crucial for spreading the gene. Various plasmid replicon types have been identified as carriers of *bla*NDM, with the e*nterobacteriaceae* group containing 20 distinct replicon types of *bla*NDM-carrying plasmids. These types include IncB/K/O/Z, IncC, IncFIA, IncFIB, IncFIC, IncFIII, IncHI1, IncHI2, IncHI3, IncL/M, IncN, IncN2, IncP, IncR, IncT, IncX1, IncX3, IncX4, IncY, and ColE10

(Baraniak et al., 2016; Yoon et al., 2018). This suggests that *bla*NDM has been acquired by various plasmids on multiple occasions, highlighting the concerning observation that numerous plasmids play a role in the horizontal transmission of *bla*NDM. We have also encountered uncertainty surrounding the precise position of *bla*CTX-M-15 inside genomes, which remains unresolved. In contrast, other β-lactamase genes were mostly identified on either the plasmid or the chromosome.

The current work also investigates the crucial inquiry of whether carbapenemase, either *bla*OXA or *bla*NDM, is responsible for elevated MIC values. Additionally, it examines if a specific pair of dual carbapenemases results in exceptionally high MIC values. Seven strains of *K. pneumoniae* were selected, characterized by the absence of carbapenemase genes, the presence of a single carbapenemase gene, or the presence of two carbapenemase genes. The genomic sequences of all isolates were examined, and no variations were detected in the mutations of porins. Furthermore, there was no notable disparity in the presence of efflux pumps among the sensitive and resistant isolates. Based on our investigation, we have determined that the carbapenemases (*bla*NDM-1, *bla*NDM-5, *bla*OXA-181, and *bla*OXA-232) are responsible for the carbapenem resistance seen in the *K. pneumoniae* isolates that were investigated. Given that the main objective of the research was to establish a relationship between the occurrence of single and dual carbapenemase producers and the MIC values, we will now proceed to explore this matter in the next section.

Klebsiella pneumoniae isolates carrying the *bla*NDM and *bla*OXA genes are often seen, and several studies have assessed the minimum inhibitory concentration of these isolates (Potron et al., 2013; I. R. Lee et al., 2016; Avolio et al., 2017; Sherchan et al., 2020; Oueslati et al., 2020). Nevertheless, while the threshold for resistant isolates is more than 2 μg/mL for ertapenem and greater than 4 μg/mL for meropenem, the majority of reports indicate resistance and levels beyond the threshold are not measured. In this work, we performed a Minimum Inhibitory Concentration (MIC) test up to a concentration of 512 μg/mL in order to identify variations among the carbapenemases.

The carbapenemases OXA-181 and OXA-232 differ by only one amino acid, with OXA-181 having arginine at position 225 and OXA-232 having serine. Despite this small difference, OXA-181-carrying isolates have high MIC values. Similarly, there are two amino acid differences between NDM-1 and NDM-5. NDM-1 has valine at the 89th position and leucine at the 156th position, while NDM-5 has leucine at the 89th position and methionine at the 156th position. Interestingly, NDM-5-harbouring isolates also exhibit high MIC values.

This little variation in amino acids, whether it be a single or double difference, may have a role in increasing the ability of carbapenemases to bind with both antibiotics. This might be the primary cause for the observed elevated MIC values. Furthermore, the analysis revealed that the isolated strain carrying OXA-181 (J20) exhibited a higher MIC, indicating a stronger hydrolytic activity against carbapenems. Recent investigations have shown that as compared to OXA-48 and OXA-181, OXA-232 exhibits less hydrolytic activity towards carbapenems but displays a greater capacity to hydrolyze penicillins (Potron et al., 2013; Oueslati et al., 2020)). In addition, the NDM-5 (M53) isolate exhibited higher MIC. Similarly, research found that NDM variants, including NDM-4, NDM-5, and NDM-7, shown increased activity against carbapenems compared to NDM-1 (Rahman et al., 2014).

Overall, NDM-5 exhibited higher MIC values (≥ 512 µg/mL) compared to the other three carbapenemase producers. Specifically, NDM-5 showed MIC values of 512 µg/mL for ertapenem and meropenem, indicating reduced susceptibility to both carbapenem drugs. Subsequently, we conducted a comparison of the dual carbapenemase producers and observed that the combination of *bla*NDM-5 + *bla*OXA-181 producer (M49) exhibited significantly higher minimum inhibitory concentration values compared to the combination of *bla*NDM-1 + *bla*OXA-232 (M17B). Research conducted in Oman, Singapore, and Norway revealed the presence of a *K. pneumoniae* strain that produces two types of carbapenemase enzymes, namely *bla*OXA-181 and *bla*NDM-1. This strain exhibited high minimum inhibitory concentration (MIC) values (>32 µg/mL) for both meropenem and ertapenem (Dortet et al., 2012; Samuelsen et al., 2013; Teo et al., 2021). Another study conducted in Nepal found that the coproducer of *bla*NDM-1 + *bla*OXA-181/232 exhibited a minimum inhibitory concentration range of 128-512 µg/mL in isolates of *K. pneumoniae* (Sherchan et al., 2020). A limitation of the current investigation is the unavailability of NDM-5 + OXA-232 and NDM-1 + OXA-181 dual carbapenemase manufacturers. Therefore, it is necessary to conduct research to have a comprehensive understanding of the full analysis of these combinations. Finally, we conducted docking tests to confirm the accuracy of our genotypic and phenotypic findings. This tool enables the analysis of the conformation and orientation, sometimes known as "pose," of carbapenem medicines inside the binding site of a large molecule target (Torres et al., 2019). Drugs with carbapenem-resistant proteins exhibiting strong binding affinity and low energy docking conformations. When compared to OXA-181, NDM-5, and NDM-1, OXA-232 showed the lowest binding energies and the highest binding affinity for meropenem and ertapenem; in contrast, NDM-1 showed the lowest binding affinity relative to OXA-232 and NDM-5. Altogether, barely any differences in binding energy were discovered for any of the

carbapenems, with the exception of OXA-232. Owing to the overuse of antibiotics, substitute therapeutic approaches are required, such as the manufacture of nanoparticles (silver, gold, etc.), quorum sensing inhibitors, and identification of new targets.

Our investigation revealed that the vast majority of the susceptible and MDR isolates belonged to less frequent sequence types. However, the XDR and PDR isolates were associated with ST231, ST147, and ST2096, which are the commonest types in India. Consistent with our research, a study demonstrated a correlation between the presence of *bla*OXA-232 genes and the XDR category (AL-Muzahmi et al., 2023; Al-Zahrani et al., 2024). In addition, there is a positive correlation between the genetic composition of the isolates and their phenotypic features. Similar finding was also reported by various research groups (Del Rio et al., 2023; Elmanakhly et al., 2024; Sid Ahmed et al., 2024). The susceptible and MDR isolates contained fewer genes and nearly no carbapenemase genes, combined with a resistance score of either 0 or 1. Whereas XDR and PDR isolates had a resistance score of either 2 or 3, with a huge number of AMR genes that can resist multiple classes of antibiotics, including carbapenems.

It is noteworthy that all isolates, regardless of their susceptibility profile, exhibited the fos gene, which imparts resistance to fosfomycin. A comparable discovery indicated that the gene encoding FosA, referred to as *fosAKP* or *fosA5*, was identified in 99.7% of *K. pneumoniae* genomes of both resistant and susceptible. This shows that the *fos* gene has become intrinsic in *K. pneumoniae* (Singkham-in et al., 2020). All isolates possessed *oqxA* genes linked to fluoroquinolone resistance; however, variability was observed in the presence of *aac(6')-lb-cr*, predominantly associated with drug-resistant isolates. Our findings were consistent with (Amereh et al., 2023), who demonstrated *K. pneumoniae* strains had *oqxA* and *oqxB* genes with prevalence of 95% and 98% respectively. Several investigations have indicated that quinolone resistance genes, including *aac(6')-Ib-cr, oqxAB, qepA,* and *qnr*, are commonly found in *Enterobacteriaceae* (Silva-Sánchez et al., 2013; Azargun et al., 2018). The *aac(6')-Ib-cr* gene codes for an enzyme that acetylates the drug, thereby diminishing the efficacy of fluoroquinolones (FQs), while the *qepA* and *oqxAB* genes facilitate the synthesis of efflux pumps, which lower intracellular concentrations of FQs (Robicsek et al., 2006; Yamane et al., 2007). Ambiguity was noted about the *tet* gene associated with tetracycline resistance, as it was not detected in all tetracycline-resistant isolates classified as XDR. Remarkably, even a limited number of isolates from the susceptible category possessed the *tet* gene, but none of the PDR isolates contained this gene. This implies that another mechanism other than *tet* gene, such as a mutation in *ramR,* could confer tetracycline resistance to *K. pneumoniae* (George et al., 1995; Grossman, 2016). The *arr-2* gene, related with rifampin resistance, was unexpectedly linked

to XDR and PDR isolates from 2020, excluding DJ, highlighting the increasing worry regarding rifampin resistance in *K. pneumoniae*. A study for Abidjan also raised concerns about the growth of the *arr-2* gene in *K. pneumoniae*, which limits treatment options because these strains are more likely to be resistant to common medicines (Gadou et al., 2018). For aminoglycoside antibiotics, the *aadA2* gene exhibited consistent presence, being identified in nearly all XDR and PDR isolates; conversely, other gene variants of *aac, aph,* and *rmt* were dispersed arbitrarily among aminoglycoside resistant isolates. Consistent with our findings, several investigations have shown the association of the *aadA2* gene with aminoglycoside-resistant XDR and PDR isolates (Quraini et al., 2023; H. Shin et al., 2023), whereas another study noted the randomized distribution of other genes among XDR and PDR conditions (X. Zhu et al., 2020).

Surprisingly, even though PDR isolates showed a colistin-resistant phenotype, they did not have *mcr* genes. In line with our results, another investigation demonstrated that the four colistin-resistant isolates, which were classified as ST-231 and ST-395, did not possess the plasmid-mediated *mcr* gene (AL-Muzahmi et al., 2023). This suggests that other factors such as mutations in *PhoPQ* and *PmrAB* operons may influence how effectively colistin drugs work as reported (AL-Muzahmi et al., 2023). Further, these mutations were examined in our isolates that was resistant to colistin, no mutation was found in the amino acid sequences of PhoPQ and PmrA in our investigation. The sole mutation, T246A, was present in another protein, PmrB, and it was shared by the isolates M47 and M50. In line with our findings This T246A mutation in colistin-resistant *K. pneumoniae* has been documented in many studies (Baron et al., 2021; Rocha et al., 2022; Basu et al., 2024; Alousi et al., 2024). Based on our finding and literature we can conclude that the mutation T246A was responsible for colistin resistance in isolate M47 and M50. However, there is another study reported across all mutations in *PmrB* gene as the second most frequent for colistin resistance after mutation or deletion in the *mgrB* gene (Yusof et al., 2022). Surprisingly, none of the two complement systems-related amino acid sequences of PhoPQ and PmrAB were mutated in colistin-resistant isolate M48, which also had the intact *mgrB* gene and was negative for the *mcr* gene. This suggests that there could be other possible molecular mechanisms that lead to the colistin resistance in isolate M48.

The *ramR* gene mutation in the context of tigecycline resistance was investigated. The most common substitution found in tigecycline-resistant isolates was valine substitution for methionine at position 184 (M184V). This mutation was also reported in Thailand (Chirabhundhu et al., 2024), and only report showed the M184V mutation worldwide as per our search. They have also reported the I141T mutation, which was also detected in one isolate

(M54) in our study (Chirabhundhu et al., 2024). The mutation I141T have also reported in other studies, and it resulted in upto 30-fold upregulation of *ramA* gene (X. Wang et al., 2015). Another mutation in our study, A19V, along with G25S, was detected in isolate M56; however, both were less frequent and restricted only to M56. The A19V mutation was shown to be most common in Taipei and China (Z.-K. Sheng et al., 2014; Chiu et al., 2017), also identified in Iran (Moghimi et al., 2021), which contrasts with our findings. Most of the isolates from Taipei with mutation A19V had another mutation, but it wasn't the same as ours, which is consistent with our findings (Chiu et al., 2017). Another study has shown that, *K. pneumoniae* strains with the mutation A19V showed 3.24–6-fold overexpression of the *ramA* gene (X. Wang et al., 2015). It was discovered that the A19V mutation was a nonsense mutation that increased tigecycline resistance (Rosenblum et al., 2011). In a different Korean investigation, investigators demonstrated a mutation in the *ramR* gene wherein valine replaced alanine and threonine replaced isoleucine. But they haven't specified where the mutation is occurring (Ahn et al., 2016). Similar alterations were also found in our investigation; at positions 19 and 173, valine replaced alanine, and at position 141, threonine replaced isoleucine. Since this I141T was not previously reported, a further investigation has identified it as a unique mutation in tigecycline-resistant *K. pneumoniae* (Moghimi et al., 2021). In the present study, we identified a mutation on position 25, where serine seems to have substituted glycine; however, this was only observed in one isolate. Comparably, a Chinese paper also reported the mutation at position 25; however, contrary to our findings, cystine replaced glycine in that location (Q. Zhang et al., 2021). As far as we can tell from our literature search, in addition to the mutations listed above, our analysis also identified a few more variants (R3S, K9I, R35C, A72P, A153T, and A173V) that had not been previously reported. The isolates in interest may have developed tigecycline resistance because of these potential new alterations. According to Villa et al., tigecycline resistance is caused by mutation in the *ramR* gene, which is a transcriptional activator of the *acrAB* genes and activates the AcrAB efflux pumps (Villa, Capone, et al., 2013).

To overcome the growing issue of bacteria that are resistant to multiple drugs and biofilm formation, this strategy suggests a new antimicrobial and antibiofilm treatment that might be used instead of traditional antibiotics. It does this by using the mechanism and selectivity of phages to kill cells (Lakshminarasimhan, 2022b). In this study, we have endeavored to use the genetic elements of the organism itself, that is the temperate phage, in the same way to address the difficulties posed by biofilm formation caused by *K. pneumoniae*. Presently, there is a

growing interest among the scientific community about alternate antibacterial agents such as bacteriophages and phage-encoded endolysins (Maciejewska et al., 2017).

Furthermore, there has been a limited amount of study conducted on the prevalence of prophages in *K. pneumoniae* species, although their significant influence on the genetic variability, evolutionary processes, and disease-causing potential of the bacterial hosts (L. Wang et al., 2017; Shen et al., 2020; Bleriot et al., 2020; Baliga et al., 2021). Based on this research, the clone ST231 was shown to be the most common in both this study and in India, with ST147 being the second most frequent. Both clones are renowned for harboring carbapenem-resistant genes (Shukla, Desai, et al., 2023; Sundaresan et al., 2022). All isolates in the genomic investigation had prophages in their genome, with a range of 1 to 6. Based on a recent examination of the variety of *K. pneumoniae* prophages, each strain was found to have between 1 and 25 prophages in total (Kang et al., 2023). This is a much higher number compared to what was seen in our research. All isolates, except for M36 and M39, showed intact prophages within their genome. To correlate the genotypic results with the actual prophage induction, all eight clinical isolates examined had intact prophages in their genome that displayed plaques, with the exception of M36, which contained just incomplete prophages. Curiously, all ST147 strains had a minimum of 5 fully functional prophages in their genome, which was a higher number compared to other STs. ST147 had a higher proportion of intact prophages and possessed both "Klebsi" and "OTK" phage types, whereas ST231 exclusively harbored OTK phages, with less intact phages and more incomplete phages. Reports indicate that incomplete and questionable prophages may be deficient in essential phage functions (De Sousa et al., 2020).

The analysis of the isolates belonging to the biofilm category revealed that the majority of them exhibited a moderate level of biofilm formation, followed by a strong level. However, an equal number of isolates showed poor biofilm formation or did not produce biofilms at all. During the growth curve assay of a few selected isolates, it was observed that all tested isolates exhibited a decrease in growth at a dose of 5 ug/ml of MMC. As a result, lower concentrations were selected for the prophage induction therapy. The analysis of the isolates belonging to the biofilm category revealed that the majority of them exhibited a moderate level of biofilm formation, followed by a strong level. However, an equal number of isolates showed poor biofilm formation or did not produce biofilms at all. During the growth curve assay of a few selected isolates, it was observed that all tested isolates exhibited a decrease in growth at a dose of 5 ug/ml of MMC. As a result, lower concentrations were selected for the prophage induction

therapy similar to mentioned by (De Sousa et al., 2020). Further, we employed the biofilm assay using MMC-containing culture to assess the influence of prophage induction on biofilm formation. Our findings indicate that, with the exception of M55 and M10, the induction of prophage is correlated with a reduction in biofilm formation. (Dakheel et al., 2019) published similar results for *Staphylococcus aureus*, demonstrating a noticeable reduction in biofilm formation when the culture was infected with phage compared to the culture that was not injected with phage. Another investigation conducted in India discovered that the utilization of both colistin and phage proved to be more effective in eradicating *K. pneumoniae* during the biofilm phase. Hence, the minimum concentrations required to eliminate biofilm (MBECs) reduced from 16–32 µg/ml to 4 µg/ml (Ragupathi et al., 2023). Furthermore, there have been reports suggesting that the induction of prophages not only reduces biofilm formation but also has the potential to enhance it, as studied in *S. pneumoniae* (Carrolo et al., 2010). Prophage induction can also happen on its own, which can lead to good competition and change how bacterial communities behave or how strong pathogenic strains are (Nanda et al., 2015).

In summary, this chapter identified ST231, ST147, and ST2096 as the most prevalent sequence types. These types were found to carry multiple carbapenemase and ESBLs genes, specifically *bla*OXA-232, *bla*NDM-5, and *bla*CTX-M-15. Carbapenemase genes were detected on plasmids, while *bla*CTX-M-15 was found on the chromosome. In addition, the impact of having both *bla*OXA-48-like and *bla*NDM-type carbapenemases in a single genome has been investigated. The study revealed that this combination may significantly increase the minimum inhibitory concentration level of carbapenem medicines to ≥ 512 ug/ml, which is matter of concern. Additional genotypic and phenotypic link was seen in laboratory isolates, where isolates with higher resistance (XDR, PDR) had a significant number of antimicrobial resistance genes, mostly associated with ST231, ST147, and ST2096. Nevertheless, the genetic material of bacteria, referred to as prophages, may be used to overcome the obstacles posed by antimicrobial resistance and virulence. Using lower quantities of mitomycin C has a limited effect in inducing the prophage, which has shown promise in reducing biofilm formation, a contributing reason to increased drug resistance.